universität wien

DIPLOMARBEIT / DIPLOMA THESIS

Titel der Diplomarbeit / Title of the Diploma Thesis

"Effect of TIP peptides on the cell surface abundance of ENaC PHA1B-causing frameshift mutants"

verfasst von / submitted by

Alina Wagner

angestrebter akademischer Grad / in partial fulfilment of the requirements for the degree of

Magistra der Pharmazie (Mag.pharm.)

Wien, 2018 / Vienna, 2018

Studienkennzahl lt. Studienblatt / degree programme code as it appears on the student record sheet:	A 449
Studienrichtung lt. Studienblatt / degree programme as it appears on the student record sheet:	Diplomstudium Pharmazie
Betreut von / Supervisor:	Ao.Univ.Prof. Mag. Dr. Rosa Lemmens-Gruber
Mitbetreut von / Co-Supervisor:	Dr. Mohammed Aufy

"Wisdom is not a product of schooling but of the lifelong attempt to acquire it."

Albert Einstein, 1954

Acknowledgement

First and foremost, I want to thank my supervisor Prof. Mag. Dr. Rosa Lemmens-Gruber. Without her my diploma thesis would not have been possible in the first place, and she has given me the opportunity to do proper scientific work. I would like to thank her very much for her support and understanding during my work in the department.

I also want to thank my co-supervisor Dr. Mohammed Aufy. Without his assistance and dedicated involvement in every step throughout the process, this thesis would never have been accomplished.

I would also like to express gratitude to all the others who worked with me in the Department of Pharmacology and Toxicology. Mostly, I want to say thank you to Mag. Dr. Waheed Shabbir, BSc MSc, who has always encouraged me throughout my studies and who has contributed a big part to the fact that my interest in research was aroused. Of course, I want to thank Anita Willam as well who always shared her time and knowledge with me. Moreover, I want to thank Mag. Shahid Iqbal.

Getting through my studies required more than academic support, and I have many, many people to thank for listening to and, at times, having to tolerate me over the past years. I would like to express my gratitude and appreciation for my boyfriend and my friends. For many memorable evenings out and in, I must thank each of you.

I must also thank my colleague Birgit, who worked on her thesis at the Department at the same time. Thanks for the entertainment and support. Without her it would not have been the same!

Mein größter Dank aber gilt natürlich meiner Familie, ohne die es mir nicht möglich gewesen wäre mein Studium zu absolvieren. Vielen Dank für die emotionale und natürlich auch finanzielle Unterstützung, ich weiß es war nicht immer ganz so einfach. Danke Mama und Papa, Bruder- und Schwesterherz, Berta Oma, Anna Oma und natürlich Opa! Ich bin ewig dankbar für eure Unterstützung.

TABLE OF CONTENTS

1 Introduction

The epithelial sodium channel (ENaC) is the limiting factor for sodium reabsorption in epithelial cells and is crucial for the maintenance of the sodium and water balance of the whole body (1). It has a wide tissue distribution (2), and its activity is affected by its cell surface expression and open probability, which are regulated by different factors like hormones, cytokines and other substances (3). Mutations, which are found in different subunits and different regions of the protein, can lead to a dysfunction of the channel and to various hereditary diseases (4–7). Loss-of-ENaC-function leads to a rare, life-threatening syndrome, called pseudohypoaldosteronism type 1B (PHA1B), which requires lifelong medical assistance (5, 8).

The lectin-like domain of the cytokine TNF-α (TIP) has shown an activation of the epithelial sodium channel (9, 10). Based on the work of *Hazemi et al*. (11), AP301 (INN: solnatide) and its congener AP318, two synthetic, cyclic peptides, which mimic TIP, have been studied how they alter ENaC function and expression (9, 10, 12, 13). TIP peptides activate the amiloride-sensitive sodium current by changing the ion channel kinetics and membrane abundance, and they restore the channel function in PHA1B-causing frameshift mutants (14).

The following overview deals with the structure, phylogeny, regulation, physiology and pathophysiology of the amiloride-sensitive sodium channel and with TIP peptides as a possible treatment for PHA1B.

1.1 ENaC – channel architecture, stoichiometry and phylogeny

ENaC, a heteromeric ion channel, is composed of four homologous subunits α, β, γ and δ (15–19) *(Figure 1).* Usually one or two α- or δ-subunits assemble with a β- and a γ-subunit to form a functional channel (16, 18, 19), but at least three subunits are needed for full activity (16, 18–20). The stoichiometry of the epithelial sodium channel is still controversial: Some research groups suggest a heterotetrametric $\alpha_2\beta_1\gamma_1$ stoichiometry (19, 21) (*Figure 1*), whereas *Snyder et al*. (22) suggest a nonameric stoichiometry of ENaC. *Firsov et al*. (4) propose a fixed heteromeric stoichiometry for ENaC when αβγ are co-expressed. They quantified the cell surface expression of ENaC by correlating the specific binding of an anti-FLAG-mAB to FLAG-tagged ENaC subunits. The ENaC activity was determined by measuring the amiloride-sensitive sodium current. Binding experiments depicted a higher abundance of the α-subunit on the

cell surface and therefore, a tetrameric formation of ENaC was proposed consisting of $\alpha_2\beta_1\gamma_1$ (19) (*Figure 1*). As in the colonic epithelial cells only the α-subunit is expressed, it is also possible that a channel is formed by only two subunits (αα) (23). The crystal structure of ENaC has not yet been determined, but according to different experimental approaches and homology models of the resolved structure of the acid-sensing ion channel 1 (ASIC1) (*Figure 2*), a heterotrimeric structure of ENaC in the plasma membrane can be deduced *(Figure 1)* (24).

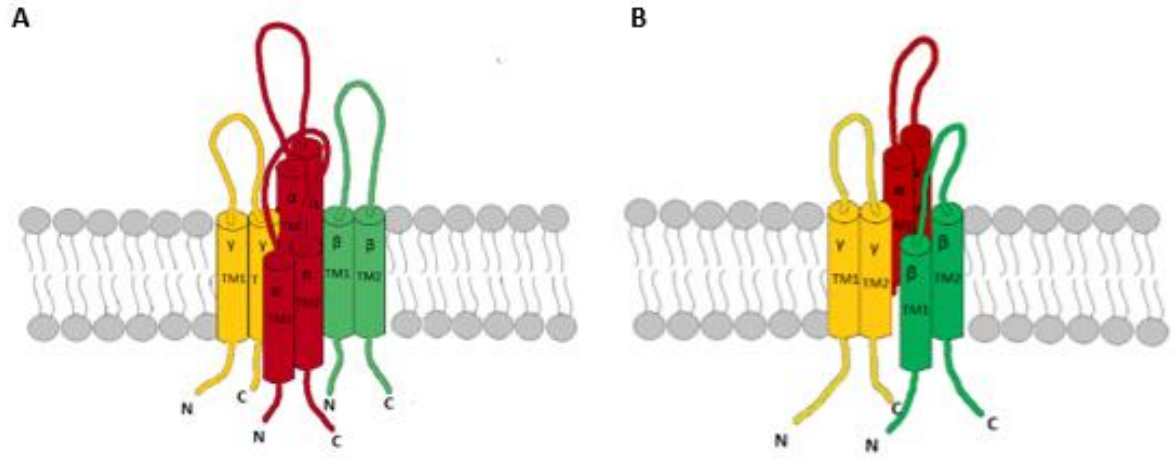

FIGURE 1. **Channel Stoichiometry.**

(A) A possible heterotetrametric structure of ENaC consisting of two α-subunits (red), one β- (green) and one γ-subunit (yellow). *(B)* A possible heterotrimeric stoichiometry.

The ENaC/DEG ion channel family members can be identified by their common topology (25), and they share an amino acid sequence identity of approximately 15–20% (24, 26, 27). The *degenerin* (DEG) gene family was identified in *Caenorhabditis elegans*: *mecs* (mechanosensation) and *degs* (neurodegeneration) (17) are involved in mechanosensation (28) and *flrs* controls the defecation rhythm (29). Moreover, a neuropeptide-gated channel was found in marine snails (FaNaC) (30).

Among mammals there are two major groups: 1. Non-voltage gated sodium channels consisting of four paralogous genes encoding ENaC proteins and 2. ASICs (acid-sensing ion channels) consisting of five paralogous genes (25).

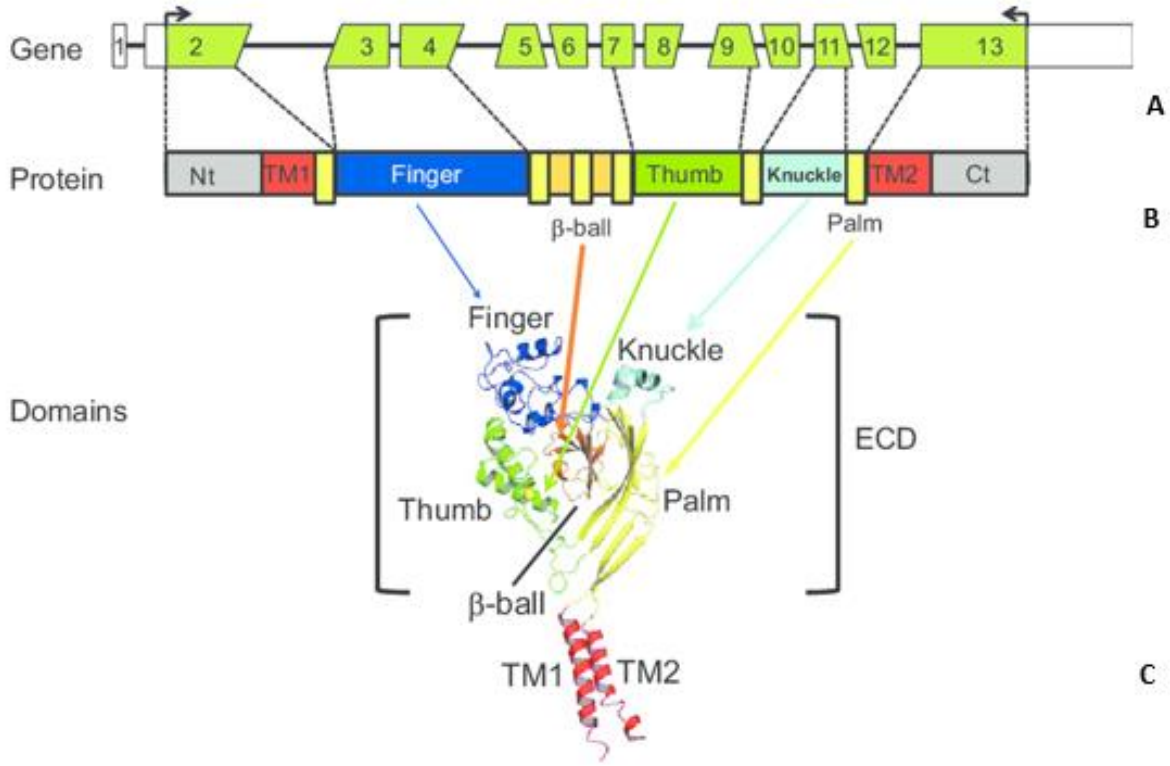

FIGURE 2. **SCNN1 gene, linear protein scheme and homology model of ENaC.**

(A) Model of a gene encoding hENaC and consisting of 13 exons. *(B)* Linear model of the ENaC protein that shows that the cytoplasmic NH_2 and COOH termini as well as the TM1 and TM2 domains are encoded by Exons 2 and 13. The major part of the extracellular loop is encoded by Exons 3 to 12. *(C)* Homology model of ENaC by reference to the resolved structure of ASIC1 (31).

A subunit resembles a forearm and a hand holding a ball. The transmembrane domain correlates with the forearm and the wrist domain (not in picture, preM2) with the connection between transmembrane and extracellular domain. The ECD (extracellular domain) consists of palm, knuckle, finger, β-ball and thumb (27, 32).

(Source: figure from (31))

ASICs assemble as a homo- or heterotrimer (33), and they are neuronal voltage-insensitive sodium channels which are also permeable for sodium and inhibited by amiloride. What can already be seen from their name is that they are activated by extracellular protons (H^+) which happens during normal synaptic transmission and acidosis (33). They are situated in the central and peripheral nervous system and react to an increase in H^+, so they are involved in pain sensation (34, 35).

Each of the four homologous genes of the cationic epithelial sodium channel (ENaC) encodes a different subunit (16, 17). SCNN1A encodes the α-subunit, SCNN1B for the β-subunit,

SCNN1G for the γ-subunit, SCNN1D for the δ-subunit (*Figure 3*). SCNN1 stands for "sodium channel, nonneural" and should be distinguished from the voltage gated sodium channel type 1 (SCN1), which is expressed in muscle and neurons (26, 36). The epithelial sodium channel is voltage insensitive. Due to the inhibition by amiloride, a potassium-sparing diuretic, it is also called amiloride-sensitive sodium channel (ASSC) (24, 36).

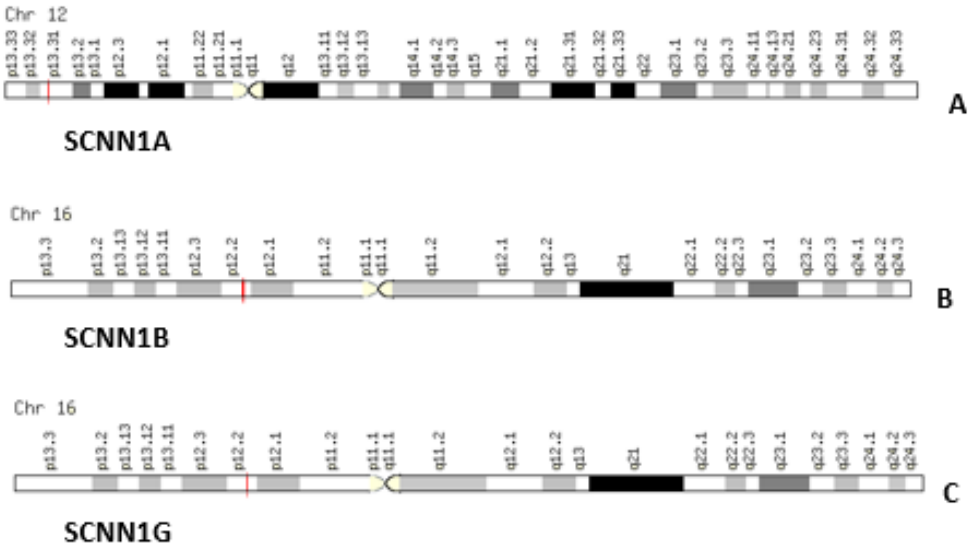

FIGURE 3. **Chromosomal location of ENaC encoding genes SCNN1A, SCNN1B, SCNN1G.**

The genes are found on the short arm (p) of their respective chromosome. *(A)* SCNN1A is located on chromosome 12 at position 13.31, while SCNN1B *(B)* and SCNN1G *(C)* are located on chromosome 16 at position 12.2. The SCNN1B and SCNN1G are very close on the same chromosome, they possibly derived from gene duplication (36).

(Source: www.genecards.org, modified)

Each of the four subunits holds a molecular mass of 85–95 kDa without any posttranslational modification, which is very important for the expression and the activity of ENaC. An overall homology of 30–40% between their primary sequences has been determined (3). The primary sequence of ENaC was best characterized and studied by expression in clones of *Xenopus leavis* oocytes (16) by sequencing the cDNA encoding the α-subunit of ENaC (36). More precisely, this sequence analysis has revealed a sequence identity between the α-, β- and γ-ENaC subunits of 29–36% (3) and a 37% identity between the α- and δ-subunit (15). The difference between the latter subunits lies in the ion selectivity since δ-ENaC is more

permeable to sodium than to lithium and α-ENaC is more permeable to lithium than to sodium (18). However, both show an impermeability to larger ions like potassium (18). ENaC, unlike the other members of the ENaC/DEG family, is more selective for sodium (Na^+) and lithium (Li^+) than for potassium (K^+) (37, 38). Responsible for this is an ion selectivity filter, which can differentiate between the size of cations and the charge of ions (anions cannot enter) (38, 39). Throughout the assembly of the subunits, the TM2 region of every subunit forms the channel pore and the selectivity filter occurs at the tightest area (40). In the preM2 segment, a Gly/Ser-X-Ser motif has been identified, which is involved in ion selectivity and also constitutes the cation binding site (38, 39). Moreover, the δ-subunit is more sensitive to the blockers amiloride and benzamil (18). This difference in amiloride sensitivity could be traced back to diverging amino acid residues of the α-subunit (Q581, W582) and δ-subunit (L581, Y582) (18). The preM2 segment of all subunits is important for the amiloride sensitivity of the epithelial sodium channel (41). Via site-directed mutagenesis, specific amino acid residues have been found in the preM2 segment of all four subunits that tend to be important for the interaction of amiloride with the channel. These are serine residues for the α- and δ-subunit and, at the corresponding positions, glycine residues for the β- and γ-subunit (38, 41). The two properties ion selectivity and pharmacology of α- or δ-ENaC do not alter when they are co-expressed with the β- and γ-subunit. Thus, it can be presumed that the α- or δ-ENaC are the pore-forming units (16, 18). The accessory β- and γ-subunits are important for ENaC trafficking (15, 16, 42). As for other membrane proteins, it is reasonable to assume for ENaC as well that the assembly of the subunits and an oligomerization in the endoplasmic reticulum (ER) are crucial before reaching the Golgi and targeting the plasma membrane (4, 43). α-ENaC or δ-ENaC alone, without the co-expression of the β- and γ-subunit, generate only a small amiloride-sensitive sodium current, presumably due to small amounts of endogenous β-ENaC- and γ-ENaC-like subunits investigated in the oocytes (18). Thus, the β- and γ-subunit are required for a proper cell surface expression and a functional ENaC protein (4). A co-expression of α-ENaC with the β- and γ-subunit leads to the same increase in Na^+-current as a co-expression of δ-ENaC with both subunits (16). The increase in the current correlates with a higher cell surface expression (4). β-ENaC and γ-ENaC alone do not produce any current (4, 16, 23).

Konstas et al. (42) suggest that the intracellular domains (C-terminus and N-terminus) and the two transmembrane domains (TM1 and TM2) in γ-ENaC are more important for ENaC trafficking and the assembly of the channel than the corresponding regions of the β-subunit.

Thus, the γ-subunit is probably more important for the cell surface expression of a functional channel than the β-subunit (42). Especially the N-terminus and the TM2 domain of γ-ENaC are important for the channel formation. If any of these two regions are missing or mutated, it will not be possible to form a functional channel and so, the function of the subunit will be disturbed (44).

A

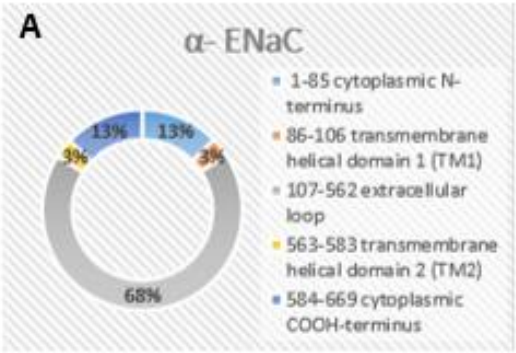

B

Amino acids	Description	Length
1-85	cytoplasmic N-terminus	85
86-106	transmembrane helical domain 1 (TM1)	21
107-562	extracellular loop	456
563-583	transmembrane helical domain 2 (TM2)	21
584-669	cytoplasmic COOH-terminus	86

***FIGURE 4.* α-ENaC topology.**

(A) Diagram created with Microsoft Excel. *(B)* Table according to uniport.org, created with Microsoft Excel (Source: https://www.uniprot.org/uniprot/P37088, modified)

A

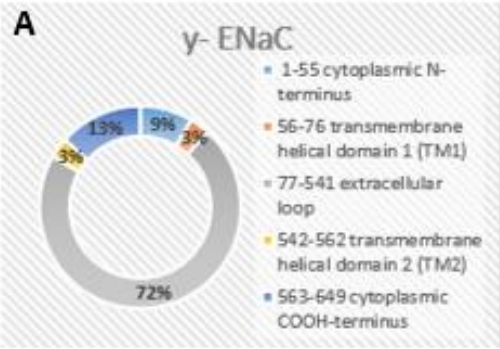

B

Amino acids	Description	Length
1-55	cytoplasmic N-terminus	55
56-76	transmembrane helical domain 1 (TM1)	21
77-541	extracellular loop	465
542-562	transmembrane helical domain 2 (TM2)	21
563-649	cytoplasmic COOH-terminus	87

***FIGURE 5.* γ-ENaC topology.**

(A) Diagram created with Microsoft Excel *(B)* Table according to uniport.org, created with Microsoft Excel (Source: https://www.uniprot.org/uniprot/P51170, modified)

Each subunit of ENaC is composed of an intracellular N- and C-terminus, two hydrophobic transmembrane helices (TM1 and TM2) and in between one big hydrophilic cysteine-rich extracellular loop. Approximately 70% of the protein mass lie in the extracellular space (24) (*Figure 4, Figure 5*). The extracellular loop is important for protein-protein interaction and for the channel to sense the extracellular environment e.g. air in alveoli, urine in distal tubule and feces in the colon (45). A different number of N-glycosylation sites has been found in each

subunit of ENaC (46). The asparagine moieties which have been found in the extracellular loop are indeed important for ENaC function (12).

Certain conserved regions *(Figure 6)* among the ENaC/DEG family are very determining for the channel function. These conserved amino acid sequences are found in the transmembrane segments and their proximity as well as in the extracellular loop. Near the TM1 segment in the cytoplasmic NH_2 terminus, there is a HG-motif (His-Gly), which is important for channel gating. The post-M1 segment is also highly conserved among all the ENaC/DEG family members (36). In the extracellular loop of the ENaC family, there are two highly conserved cysteine-rich domains: CRD II and CRD III. A third cysteine-rich domain (CRD I) has been found in degenerins only (36, 45).

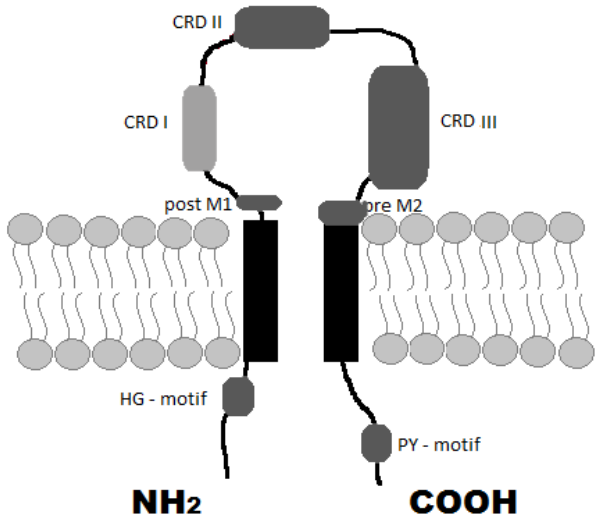

***FIGURE 6.* Localization of conserved regions in ENaC.**

The motifs shown in this scheme are well conserved among all members of the ENaC/DEG family. Except the CRD I, which is only found in degenerins, and the proline-rich domain in the cytoplasmic C-terminus, which is exclusively conserved within ENaC paralogs.

(Source: figure created according to localization of conserved regions from (36, 45))

A replacement of cysteine residues in the extracellular loop with alanine or serine affects the channel assembly and the transport to the cell surface which leads to a decrease in the cell surface expression (45). Mutations such as αC133Y cause PHA1B (pseudohypoladosteronism-1) due to the impossibility of N-linked glycosylation (45). Moreover, these residues may be important for the formation of disulfide bonds to maintain the tertiary structure of the channel respectively the extracellular loop (36). The conserved amino acid sequence PPPxYxxL, known as PY motif, is a proline-rich segment which is only conserved in the ENaC subfamily. It is found in each ENaC subunit in the cytoplasmic C-terminus (47). This PY motif is necessary for Nedd4, a ubiquitin-protein ligase, to inhibit ENaC by decreasing the cell surface

expression due to a higher rate of degradation of the protein complexes (48). The conserved amino acid residues in the pre-M2 segment prior to the transmembrane domain 2 (TM2) are important for ion permeation and the channel block by amiloride (36, 41).

1.2 ENaC – physiology and tissue distribution

The assembly of ENaC differs depending on the physiological conditions and tissue type (2). α-, β- and γ-ENaC are highly expressed in epithelial cells, especially in the kidney, lung and colon (49). The δ-subunit is mainly found in non-epithelial tissues like brain, pancreas, testis, and ovary, but it is also slightly expressed in lung and kidney (15, 18). The δ-subunit can form channels alone or in combination with the β- and γ-subunit. The δ-ENaC gene (SCNN1D) occurs in humans and guinea pigs but is absent in rats and mice (15). The differences between the α- and the δ-subunit are not only the tissue type where they are expressed in, but also the channel properties (15, 18).

The ENaC protein is located in the apical membrane of epithelial cells in the alveoli, distal nephron, collecting duct, distal colon, urinary bladder, sweat and salivary glands (1). It mediates the sodium transport through epithelial tissues and works in conjunction with the Na^+/K^+-ATPase, which is located basolaterally *(Figure 7).* The glycoprotein is very important for the regulation of the salt and water homeostasis because it is the limiting step of the sodium absorption (1). Therefore, ENaC in the kidney (and colon) plays an important role in the control of the whole body extracellular fluid volume and subsequently in the regulation of blood pressure (36). In addition, it is involved in taste perception (50) and the regulation of the lung alveolar fluid homeostasis and mucociliary clearance (36). ENaC function is physiologically very important, since genetic mutations are associated with serious hereditary conditions like Liddle's syndrome (4), cystic fibrosis (6), pulmonary oedema (7) and pseudohypoaldosteronism type 1 (PHA1) (5).

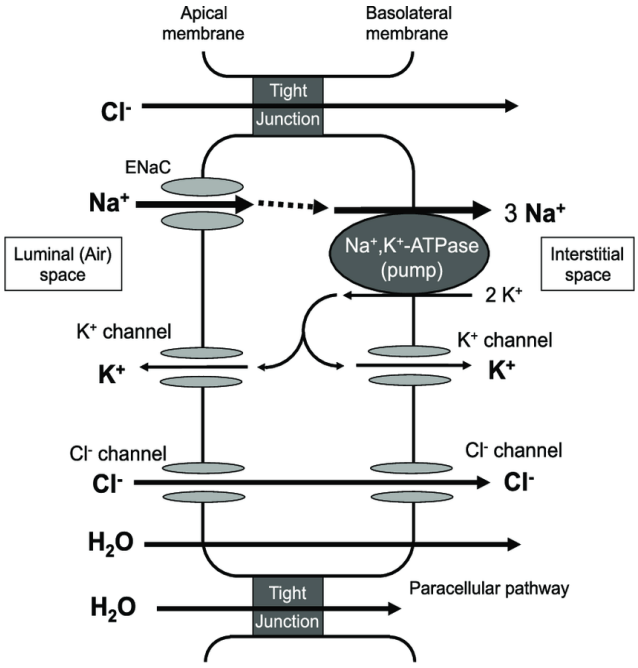

FIGURE 7. **ENaC in charge of sodium transport across epithelial cells.**

The amiloride-sensitive sodium channel allows transepithelial sodium transport across epithelial cells. It is located on the apical membrane, where it allows Na^+ from the extracellular space to enter the cell. The basolateral Na^+/K^+-ATPase is important for the maintenance of the electrochemical gradient by pumping out 3 Na^+ and ingesting 2 K^+. Sodium enters the cell and water follows sodium transcellular via osmosis through aquaporins (only in presence of vasopressin) or paracellular through tight junctions.

(Source: figure from (51))

1.3 Regulation of ENaC and biophysical properties

The activity of the epithelial sodium channel is affected by two things: cell surface expression and open probability (P_o) (1, 52). These are regulated by ubiquitination, proteolytic cleavage and other posttranslational modifications (3, 18).

1.3.1 Regulation of expression via hormones and degradation

Aldosterone (53) and vasopressin (54) are the regulators of ENaC expression in the distal nephron as well as endothelin (55) and insulin (56).

The mineralocorticoid aldosterone binds to the mineralocorticoid receptor (MR) which translocates into the nucleus and acts like a transcription factor. It induces the expression of two proteins: SGK1 (serum and glucocorticoid-regulated kinase 1) (57) and GILZ1 (58) (glucocorticoid-induced leucine zipper protein 1), both leading to a higher abundance of the epithelial sodium channels in the apical membrane. Insulin is also an inducer of the SGK1 (56). SGK1 belongs to the subfamily of the serine/threonine kinases and has a PY motif as well as ENaC. It phosphorylates the ubiquitin-protein ligase Nedd4-2 on two phosphorylation sites, both are serine residues (57). Therefore, Nedd4-2 is no longer able to interact with the conserved PY motif in ENaC. This prevents the channel protein from the ubiquitination by

Nedd4-2 and consequently from the channel degradation, which results in a higher expression of ENaC on the cell surface.

The ubiquitination, a posttranslational modification, regulates the cell surface expression of ENaC (36, 59) *(Figure 8)*. As previously described, ENaC is a substrate of the Nedd4-2 and they interact via PY motifs/WW domain (59). This PY motif is conserved among all subunits of ENaC in the cytoplasmic carboxy-terminus and plays a crucial role in the pathophysiology in Liddle's syndrome, where a truncated carboxy-terminus in the β- and γ-subunit leads to a gain-of-function of ENaC, since an ubiquitination and further degradation of ENaC surface proteins is not possible (60, 61). The PY motif consists of two proline-rich segments, P1 and P2, and Nedd4-2 interacts with the P2 region (60, 62). Nedd4-2 is composed of a N-terminal C2 domain (Ca^{2+}-dependent lipid binding domain) for targeting Nedd4-2 to the plasma membrane, a C-terminal HECT domain (the catalytic ubiquitin-protein ligase domain) and three (in rat and mouse) to four (in human) WW domains (protein-protein interaction domains). The ubiquitination of ENaC is not only performed by the required HECT domain of Nedd4-2 (59, 60), but N-terminal lysine residues in the α- and γ-subunit interact with ubiquitin as well (63). The polypeptide ubiquitin is a signal for degradation by the lysosome and proteasome. Therefore, it regulates the membrane abundance. ENaC is a short-living glycoprotein with a half-life of approximately an hour, which is also typical of ubiquitinylated proteins (64, 65). Nedd4-2 is mobilized to the membrane in a calcium-dependent manner via its C2 domain, which binds phospholipids in the membrane (66). After ENaC is retrieved from the membrane, it can either degrade or move into a recycling pool from which it can re-locate into the apical membrane (67, 68).

Aldosterone also interferes with the Raf-MEK1/2-ERK1/2 signalling pathway (58). Raf-1 (C-Raf), also a serine/threonine kinase, reduces the cell surface abundance of ENaC by activating ERK1/2, which phosphorylates the channel protein. Due to this phosphorylation, the interaction between the epithelial sodium channel and Nedd4-2 is enhanced, which leads to the degradation of the channel (69).

GILZ1 blocks Raf-1 hence inhibits the ERK1/2 signalling (58). In this way, GILZ1 increases the cell surface expression of ENaC by inhibiting the Raf-MEK1/2-ERK1/2 pathway (58). GILZ1 does not only prevent the epithelial sodium channel from phosphorylation by ERK1/2 and thereby precludes ENaCs interaction with Nedd4-2. GILZ1 also enhances the interaction of SGK1 with

Nedd4-2, which again leads to a decreased interaction of ENaC with Nedd4-2 (70). GILZ1 and SGK1 can act synergistically to inhibit Nedd4-2 (70).

Vasopressin and its second messenger cAMP (cyclic AMP), which activates PKA, increase the amiloride-sensitive conductance of the apical membrane because of a higher number of ENaC proteins (71). Cyclic AMP increases ENaC trafficking to the cell surface (67, 71). Aquaporins-2 colocalize with ENaC in the collecting duct (CD) and connecting tubule (CNT) in the kidney (72). Consequently, the presence of vasopressin respectively cAMP leads to a higher cell surface abundance of ENaC and a higher expression of aquaporins (64).

Aldosterone affects the expression of the subunits in a tissue-specific manner. In the kidney, the number of α-subunits is the limiting factor for membrane trafficking because aldosterone only increases the expression of the α- ,not the β- or γ-, subunit. In the rat colon, by contrast, the β- or γ-subunit are more expressed than the α- subunit under the influence of aldosterone (73, 74).

1.3.2 Activation of ENaC by proteolysis

Proper membrane trafficking is a crucial factor for maintaining the ENaC activity. All subunits must preassemble into a complex before targeting to the membrane (4, 44, 71). The transport of ENaC from the ER to the Golgi is carried out in an inactive form (75). In the Golgi, the channel undergoes proteolytic processing which leads to an activation of the channel protein and an increase in P_O (76). More precisely, furin, a protease, cleaves specific sites extracellularly in the α- and γ-subunits (75). But ENaC can be processed (from proprotein to active protein) by other serine proteases as well, like prostasin (cleaves γ-ENaC) (77) or plasmin (78). The cleavage results in a release of inhibitory peptides, which, in turn leads to an increased P_O. (79). Nevertheless, a small amount of ENaC proteins is not cleaved and stays inactivated (80). Channel proteins from this inactive pool can be cleaved and hence activated, if needed, by extracellular or membrane-associated enzymes such as channel-activating proteases (81). As mentioned above, cAMP increases the channel trafficking to the cell surface (67, 71). These channels derive from the recycling pool (67) and are newly synthesized as well (82).

The open probability (P_O) is impacted by either proteolytic cleavage, which leads to activation (76), or by an alternation in channel gating (83). ENaC is consecutively active (84), and its open probability varies from <0.1 to 0.9. In virtue of the differences in P_O, different channel gating modes can be deduced. These active channels can be classified into two groups: one with a

high P_O and long open times and the other with a low P_O and a long closed time (83). High extracellular sodium affects the P_O negatively by the so-called Na^+ self-inhibition (85). Intracellular sodium leads to a feedback inhibition on the channel (1).

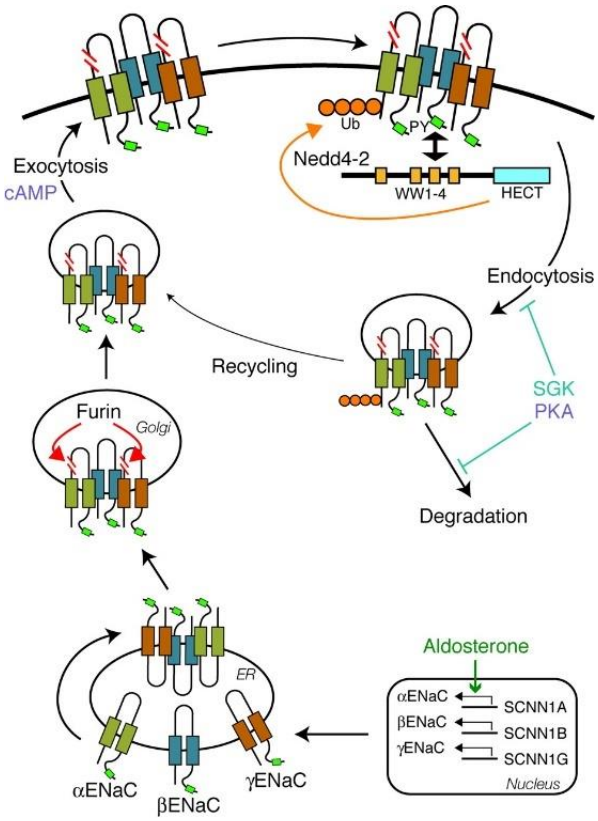

FIGURE 8. **Molecular pathway of ENaC regulation.**

Aldosterone in the kidney increases transcription of α-ENaC. The subunits assemble in the ER and migrate to the Golgi where ENaC is activated via proteolytic cleavage by furin. Then the protein targets to the membrane where it is ubiquitinylated by Nedd4-2. Subsequently, ENaC degrades. Cyclic AMP/PKA increases cell surface abundance (vasopressin→cAMP→PKA). PKA phosphorylates and therefore activates SGK1 which, in turn, inactivates Nedd4-2 through phosphorylation. In addition, cAMP/PKA phosphorylates and inhibits Nedd4-2 independently of SGK1. Aldosterone not only induces ENaC genes but also SGK1 which phosphorylates Nedd4-2. The latter is no longer able to interact with ENaC and thus the degradation is reduced.

(Source: figure from (86))

1.3.3 Regulation of ENaC by extracellular H^+, Cl^- and other factors

The extracellular domain can sense changes in pH and in the ion concentration of Na^+ and Cl^-, the two principal components of the extracellular fluid, and of metal cations like Zn^{2+} and Ni^{2+}, which alter the activity of ENaC (87, 88). Cl^- inhibits ENaC by enhancing the Na^+ self-inhibition (87). This Na^+ self-inhibition, however, is eliminated by extracellular Zn^{2+}, whereas Ni^{2+} inhibits ENaC activity. Both are dependent on the extracellular sodium concentration (88).

Changes in the pH affect ENaC gating as well by regulating the Na^+ self-inhibition: acidic pH increases the P_O by reducing the Na^+ self-inhibition, whereas alkaline pH reduces the P_O (89).

ENaC reacts to mechanical stimuli (shear stress) with increased activity. First shown in murine αβγ-ENaC (90), the activity increase is not due to a higher cell surface abundance, but is caused by a higher P_O (91). δβγ-ENaC was also investigated and showed an increase in P_O too but in lesser extent, possibly because δβγ-ENaC already has a higher intrinsic P_O (92). This thought is supported by *Carattino et al.* (91), who inserted mutations into the channel pore causing a higher P_O, whereby the channel could no longer be activated by mechanical stimuli. The mechanosensitivity of ENaC is probably the reason why a gain-of-function is seen in cystic fibrosis (CF) patients. The shear forces acting on the epithelia are higher, the more viscous the ASL (airway surface liquid) is (93).

1.3.4 Regulation of ENaC by TNF-α and by its lectin-like domain

While TNF-α decreases the expression of the epithelial sodium channel (94), its lectin-like domain (TIP) shows ENaC activating properties (9, 10).

Before targeting to the plasma membrane, the subunits of ENaC assemble in the ER and undergo N-linked glycosylation (46). Asparagines within the certain consensus sequence Asn-X-Ser/Thr (X= all amino acids except proline) are able to interact with proteins from the extracellular matrix (46). The number of putative N-linked glycosylation sites in the extracellular loop differs according to the subunit. Five of the seven sites from α-hENaC and four of the five sites of δ-hENaC are in the extracellular loop, whereas all the eleven sites of β-hENaC and all the five sites of γ-ENaC are extracellular (*Appendix_9.1. Amino acid sequences of ENaC subunits and marked glycosylation sites*). *Snyder et al*. (46) found out that the N-glycosylation is not essential for the channel function and channel processing in rat α-ENaC and since ENaC subunit orthologs have high sequence similarity, we can expect this as well for the human ENaC. This was confirmed by *Shabbir et al.* (12) by removing N-glycosylation sites. Moreover, they showed that these N-glycan moieties are important for the hENaC activation through solnatide (AP301). AP301 not only interacts with ENaC via N-glycans, but also by binding to the carboxy-terminal domain (95). This was validated by *Shabbir et al*. (12) by inserting a stop codon to delete the carboxy terminus which resulted in a not significantly enhanced whole-cell sodium current of the mutated α-ENaC by AP301. Solnatide increased the activity of the epithelial sodium channel by an alternation of ion channel kinetics in the

plasma membrane, more precisely by an increase in P_O (12, 96) as well as by a transiently increased expression of ENaC (12, 95). By eliminating the N-glycosylation sites, the solnatide-induced, transiently increased expression of α-ENaC was reduced or abolished (12).

1.4 TNF lectin-like domain peptides AP301 and AP318

TNF-α, a cytokine which plays an important role in inflammation, is produced in different kinds of cells like macrophages, lymphocytes, monocytes, fibroblasts and endothelial cells (97). The effect of TNF-α on ENaC has been shown in different studies: it decreases the expression of ENaC (94). TNF-α has often been analysed, and studies have shown that its lectin-like (TIP) domain stimulates the amiloride-sensitive sodium current of ENaC in A549 cells (10) and microvascular endothelial cells (9). Consequently, the demand for a new peptide was there, without the negative characteristics of TNF, but with the properties of the lectin-like domain (TIP) regarding the epithelial sodium channel. In this work, the effect of the TIP-mimicking cyclic peptides AP301 (solnatide) and AP318 on the cell surface expression was investigated.
The lectin-like domain, residues C101–E116 of wild type hTNF-α, has the ability to bind lectin-like oligosaccharides like N, N'-diacetylchitobiose or branched trimannoses (98). These kinds of N-glycosylation sites are found in ENaC and therefore, the lectin-like domain can activate the channel by binding on these sites in the extracellular loop (96). AP318 is characterized by a lacking disulfide bond for more stability and for a better use as a human therapeutic other than the original TIP peptide. It contains a disulfide bridge that not only leads to instability, but is not common in therapeutic compounds either (11). Moreover, a cyclisation via an amid-bound was achieved and a fundamental finding has been made: essential for ENaC activation is a free positively-charged N-terminal amino group on residue 1 or a free negatively charged carboxyl group on residue 17. However, when both charged groups are present ENaC activation is not as effective as if only one charged group is present (11).
In AP301, the cysteine at position 101 was replaced by a glycine and in addition, in the N-terminus as well as in the C-terminus, a cysteine was added. Both cysteines are linked via a disulfide bridge which results in a 17-residue cyclic peptide: Cyclo(C**G**QRETPEGAEAKPWYC) (11) *(Figure 10)*. Additionally, it has residues essential for chitose-binding and ENaC activation: T6, E8, E11 which correspond to the residues of hTNF-α T105, E107, E110, and are found on the tip of the molecule (9, 98). This leads to the finding that the hexapeptide sequence TPEGAE is crucial for binding oligosaccharides (11). The hydrophobic region P133, W114, Y115 in hTNF-

α, which is equivalently found in AP301, is also important for ENaC activation (11). Solnatide has two charged groups: a free amino group on residue 1 (residue 1 is equivalent to hTNF-α P100) and a negatively charged carboxyl group on residue 17 (11). *Hazemi et al*. (11) found out that, when two charges are present, the potency of ENaC activation is lower (EC50 ~ 54 nM for AP301, EC50 ~ 24 nM for AP318), which makes AP318 the more potent TIP peptide. *Shabbir et al*. (96) treated A459 cells, which endogenously express ENaC, with PNGase F to remove almost all potential N-linked glycosylation sites. After the treatment with AP301, the increased amiloride-sensitive sodium current could not be measured anymore. Thus they deduced that the glycosylation sites in the extracellular loop are crucial for the interaction of solnatide with ENaC. In another study *Shabbir et al*. (12) verified the findings by mutating the potential N-glycosylation sites (asparagine to glutamine) in the extracellular loop of α-ENaC. After applying solnatide, the amiloride-sensitive current was decreased and the EC50 was increased compared to the non-mutated wild type (WT) ENaC (12). In the same study, they concluded that the carboxy terminus is also crucial for solnatide to increase the sodium current (12). *Czikora et al.* (95) came to the same conclusion. Moreover, the cell surface expression of endogenous α- and δ-hENaC (in A459 cells) was only transiently increased after the treatment with solnatide as it decreased after 30 minutes, which indicates that only the translocation to the cell membrane and not the expression is increased (12). Solnatide is being developed as a therapy for various forms of pulmonary oedema. It has received orphan drug designation status in Europe for high altitude pulmonary oedema (99), pseudohypoaldosteronism type 1B (100, 101) and primary graft dysfunction (100), a complication after lung transplant within 72 hours following. Moreover, it has passed phase IIa clinical trials for the treatment of acute respiratory distress syndrome (99).

In AP318, the cysteine in position101 was replaced by a glycine as well, but in the N-terminus a 4-aminobutanoic acid and in the C-terminus an aspartic acid was added. They form an amid bond and result in a cyclic peptide: Cyclo(4-aminobutanoic acid-**G**QRETPEGAEAKPWYD) (11) *(Figure 10)*. *Shabbir et al*. (96) performed patch clamp experiments with AP318 and found out that the single channel open probability of ENaC increases after the treatment with the peptide. AP318 has been granted orphan drug designation in Europe for the treatment of PHA type 1B as well (101).

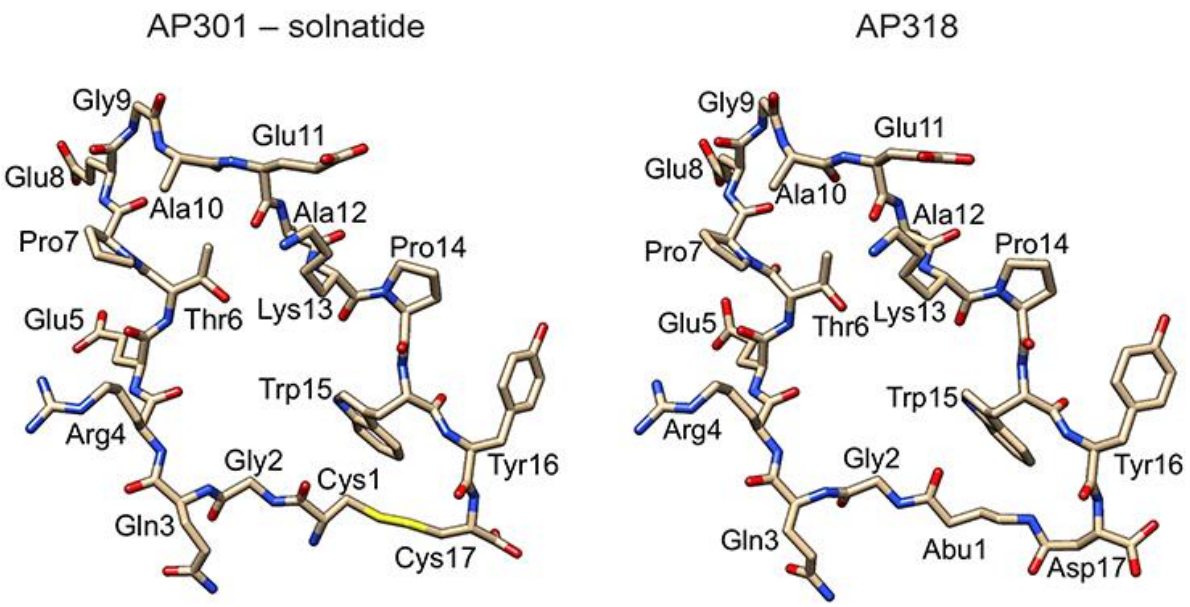

FIGURE 9. **Structure of the cyclic peptides AP301 and AP318.**

The yellow coloured part in the molecule AP301 shows the disulfide bond between two cysteine residues, C1 (C101 in TNFα) and C17 (E116 in TNFα) that permits cyclisation.

(Source: peptides modelled by (14) after previous description (11))

1.5 ENaC – Channelopathies

Mutations in genes encoding ENaC subunits lead to a functional disturbance in different kinds of tissues such as kidney, colon, and lung. Dysfunction in renal ENaC induces pseudohypoaldosteronism (5) and Liddle's syndrome (4), as ENaC controls sodium absorption and blood volume (1). Negatively affected sodium absorption in the colon (low ENaC expression) is associated with ulcerative colitis and diarrhoea (102). Pulmonary dysfunctions like cystic fibrosis and pulmonary oedema are also caused by either a loss of function (pulmonary oedema) (7) or a gain of function mutations (CF) (6) in ENaC.

1.5.1 Multi-system form of pseudohypoaldosteronism type 1 (PHA1B)

Pseudohypoaldosteronism type 1 is a hereditary, salt-wasting disorder which results in hyponatremia and consequently in hypovolemia, hyperkalaemia and metabolic acidosis (5). This rare disease is present in the neonatal period and responsive for failure to thrive, dehydration, hypotension and vomiting (103). The disease is marked by elevated renin and aldosterone levels reflecting an unresponsiveness to mineralocorticoid hormones in the kidney and other tissues (5).

Two subtypes of PHA type 1 can be differentiated: the renal form and the systemic type. These two types vary, inter alia, in genetic inheritance, mutated genes and sodium requirements (5).

The renal form is caused by mutations in NR3C2 (Nuclear receptor subfamily 3, group C, member 2), a gene encoding the mineralocorticoid receptor (MCR), and is autosomal dominant inherited (103). As previously described, aldosterone is the main regulator of ENaC activity. It increases the expression of ENaC subunit genes and thus, the sodium absorption in the distal nephron (104). Mutations in NR3C2 cause hyponatremia, hyperkalaemia with elevated renin and aldosterone levels due to a stimulated renin-angiotensin system (104). Therefore patients with PHA1 receive a supplement of oral sodium chloride (5, 8). Due to a lack of response of the MCR to aldosterone, oral aldosterone treatment is obviously not working. This form is progressing mildly and even ends in spontaneous remission with age (8).

The more severe systemic type (PHA1B) is caused by mutations in genes encoding subunits of the amiloride-sensitive epithelial sodium channel and has an autosomal recessive inheritance (5, 103) with manifestation persisting into adulthood (105). ENaC is not only present in the kidney but also in sweat and salivary glands, lungs and colon. As the latter tissues are affected as well, patients can suffer frequently from lower respiratory tract infections and consequently have similar treatment as cystic fibrosis patients. Elevated levels of sodium chloride in sweat, stool and saliva can be used for diagnosing the systemic type of PHA1 or to differentiate it from renal type (106). PHA type 1B patients receive intensive i.v. fluid and electrolyte therapy. An ion exchange resin is required to decrease the strongly elevated potassium levels (107).

Previously described frameshift mutations, which result in a loss-of-function of ENaC, are located on the SCNN1A, SCNN1B or the SCNN1G genes (108). These genes encode the subunits α (SCNN1A), β (SCNN1B), γ (SCNN1G). Human SCNN1A is assigned to chromosome 12p13 and human SCNN1B and human SCNN1G are assigned to chromosome16p12-13 (109) (*Figure 3)*. Through homozygosity mapping, a previous study found out that the gene loci responsible for PHA1 (16p12.2–13.11 in six families and to 12p13.1 in other five families) are the same loci where the genes encoding the three subunits of hENaC are located (108) (*Figure 3)*. A mutation (G37S) causing PHA1B has led to the conclusion that a conserved glycine, which is present in the cytoplasmic amino-terminus of all ENaC gene family members, reduces the open probability (P_o) of ENaC and thus is involved in the gating control of the channel (110, 111). This was observed in *Xenopus leavis* oocytes where the amino acid exchange (G37S) in

the β- (110) as well as in the α-subunit and γ-subunit led to a reduction in the sodium current compared to wild-type channel (111). Both mutant and wild-type had the same cell surface expression, single channel conductance and ion selectivity. Therefore, one can assume that the activity of ENaC was reduced but there is no complete loss of function (111).

1.5.2 Liddle's syndrome

Another rare disease, which is caused by mutations in the epithelial sodium channel, is Liddle's syndrome. It is an autosomal dominant inherited form of salt-sensitive hypertension with an early penetrance (112). Mutations in the genes encoding the β- and γ-subunit (SCNN1B, SCNN1G) lead to a gain of function in the epithelial sodium channel (61, 113). This causes an increase in sodium and water absorption and at the same time an increase in potassium secretion (61, 113). The pathological consequences are hypertension, hypokalaemia, metabolic alkalosis and low plasma aldosterone and renin levels (112). Accountable for this gain of function are mutations that lead to a truncated or deleted cytoplasmic carboxy-terminus. More precisely, a conserved region, the proline-rich PY motif in the C-terminus, is affected by mutations that cause Liddle's syndrome (61, 113). The ubiquitin-protein ligase Nedd4-2 normally binds to the PY motif of cell surface ENaC and is responsible for its endocytosis and lysosomal degradation. In the case of Liddle's syndrome, as the carboxy-terminus is truncated or even deleted, no ubiquitination is possible and therefore, more channels are found on the cell surface (60). Not only a lack of channel degradation but also an elevated channel open probability is the reason for a gain of ENaC function (4).

1.5.3 Cystic fibrosis and pulmonary oedema

ENaC is negatively regulated by activated CFTR (cystic fibrosis transmembrane conductance regulator) (6), a cAMP-activated chloride channel which is located in the apical and basolateral membrane of epithelial cells (114). More precisely, elevated chloride levels in cystic fibrosis (CF) lead to an inhibition of ENaC, as anions are an inhibiting factor of ENaC (6). In CF, CFTR is not functioning properly. Therefore, ENaC is not properly regulated which results in a gain of ENaC function. The consequence is a decrease in chloride secretion and an increase in sodium and water absorption which leads to higher mucus viscosity and decreased mucociliary clearance associated with a higher incidence of bacterial infection (115).

On the contrary, a loss of ENaC function in the alveoli leads to pulmonary oedema due to an extended airway surface liquid volume (7), as the sodium absorption and the alveolar fluid clearance are decreased (116). Therefore ENaC is crucial for airway fluid clearance (116). Indeed, PHA1 patients have an ASL volume twice as normal (117). Pulmonary oedema is part of the recovery phase of acute lung injury/acute respiratory distress syndrome (118). Moreover, high-altitude pulmonary oedema patients also show a decrease in ENaC function (119).

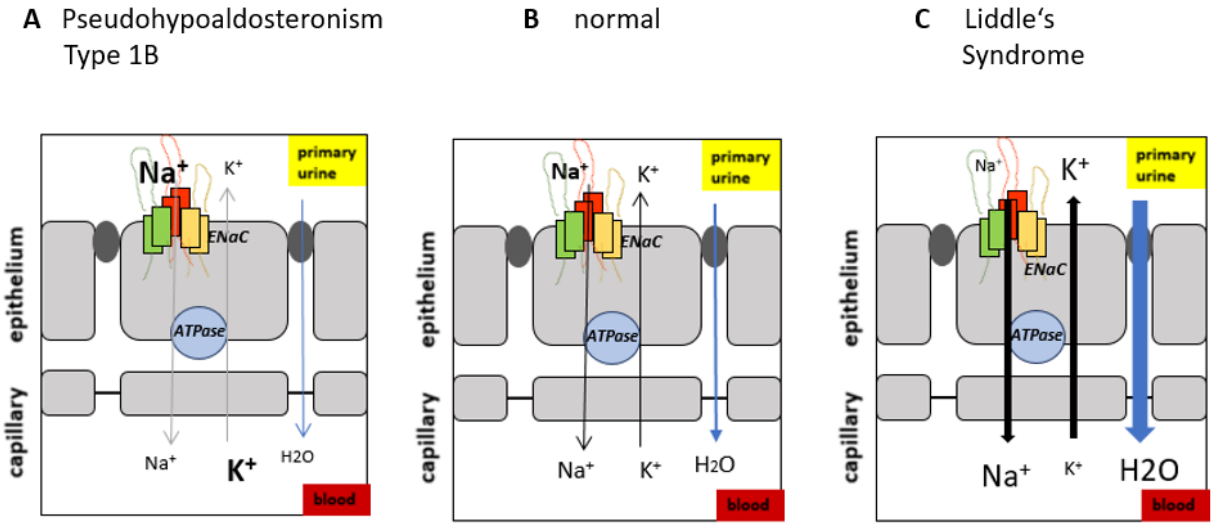

FIGURE 10. **Normal function of renal ENaC and pathophysiological changes in the kidney.**

(A) A loss-of-function in ENaC that causes pseudohypoaldosteronism type 1 leads to decreased sodium and water reabsorption in the kidney and therefore to an increased loss of electrolytes and water, which results in hypotension (5). *(B)* Normal ENaC function: Apical sodium absorption and basolateral ATPase activity lead to reabsorption of sodium from primary urine in the blood and to passive reabsorption of water due to an osmotic gradient. *(C)* A gain-of-ENaC-function, which is the reason for Liddle's syndrome, leads to an increase in sodium and water reabsorption which results in a higher blood volume and consequently hypertension (4).

(Source: (120), modified)

1.6 PHA1B-causing frameshift mutations

Mutations on the SCNN1A, SCNN1B and SCNN1G genes resulting in a loss of ENaC activity are responsible for PHA1B (108). That is why I had a closer look at the following mutations causing a frameshift error, which have been reported to cause PHA1B: γV543fs, αY447fs, αS243fs, αP197, αR438fs.

Most of the mutations causing PHA1B appear in the α-subunit (*Figure 11*). Therefore, an important role in the regulation of ENaC function can be attributed to this subunit, which has been confirmed in different studies (16, 17, 19, 21, 121).

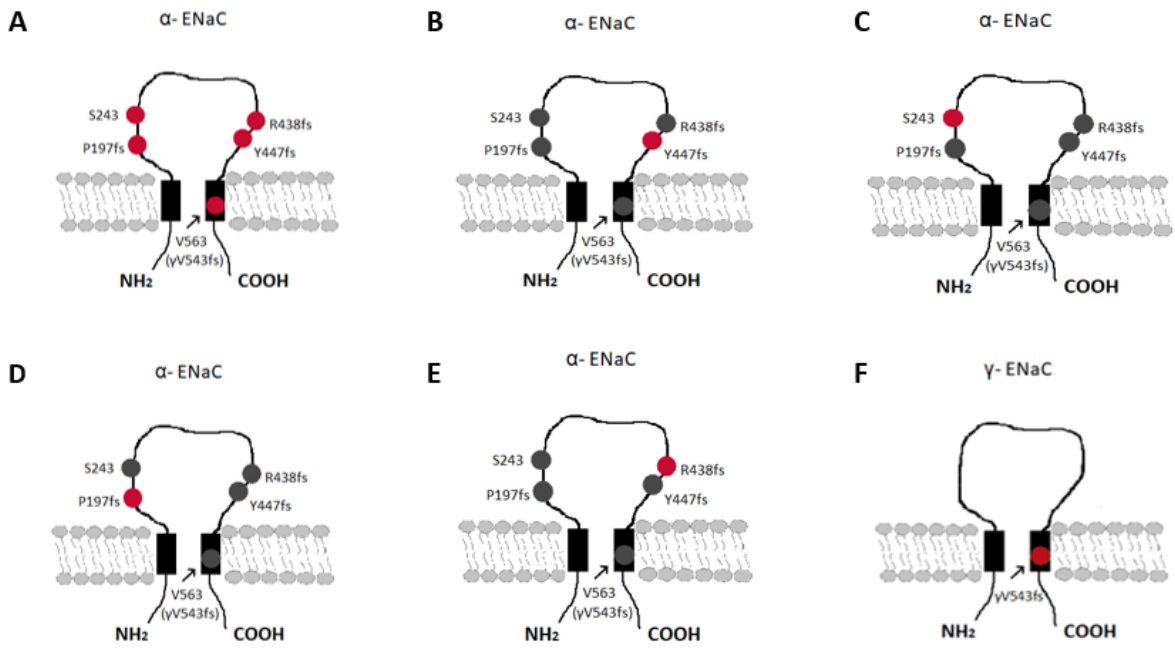

FIGURE 11. **PHA1B-causing mutants located onto ENaC.**

Schemata of approximate topological position of PHA1B mutants onto the α-/γ-subunit of ENaC according to UniProtKB - P37088, SCNNA_HUMAN; UniProtKB - P51170, SCNNAG_HUMAN. The position of the mutation in the γ-subunit is in brackets, relevant for (A), (B), (C), (D) and (E). *(A)* All the observed frameshift mutants of α-ENaC are in the extracellular loop, whereas the frameshift mutant of γ-ENaC is in the TM2. *(B)* αY447fs mutant (red) *(C)* αS243fs mutant (red) *(D)* αP197fs mutant (red) *(E)* αR438fs mutant (red) *(F)* γV543fs mutant (red)

TABLE 1. Position of mutations on gene and in protein proofed to cause PHA1B

MUTATION (PROTEIN)	*MUTATION (GENE)*	*LOCATION OF MUTATION*	*ETHNICITY*	*TRUNCATED LENGTH (PROTEIN)*
αY447fs	Exon 8, 1340insT	extracellular loop	Pakistani	458
αS243fs	Exon 4, 828delA	extracellular loop	Swedish	246
αP197fs	Exon 3, 587–588insC	extracellular loop	Turkish	204
αR438fs	Exon 8, 1311delG	extracellular loop	Chinese	480
γV543fs	Exon 13, 1627delG	TM2	Japanese	597

αY447fs

This mutation has been reported to cause PHA1B in a Pakistani patient. The patient's parents were consanguineous, and the mutation was homozygous. The insertion of a thymidine in exon 8 (1439insT) of the α-subunit gene (TAC to TTAC) leads to a frameshift mutation (Tyr447) which results in a premature stop codon (K459) (*Table 1*) (107).

This in turn leads to a truncated α-subunit more precisely to a lack of the carboxy-terminus which previously has been reported to be important for the interaction of the TIP domain with ENaC (95, 122). This mutation is located in the extracellular loop (*Figure 11B*) in the thumb domain (123). The truncated length of the protein is 458 amino acids with an approximately calculated molecular weight of 64,86 kDa.

αS243fs

The deletion of an adenine in Exon 4 (729delA) of the α-subunit gene leads to a frameshift at position S243 which results in a premature stop codon four amino acids after this position (124). This homozygous mutation was found in a Swedish patient (*Table 1*) (124). It is situated in the extracellular loop (*Figure 11C*) in the finger domain (14). The truncated length is 246 amino acids and the approximately calculated molecular weight is 34,41 kDa.

αP197fs

The insertion of cytosine between the codons 587 and 588 in exon 3 (587-588insC) of the α-subunit gene leads to a frameshift at position P197. This homozygous mutation causing a premature stop codon at position 205 results in a lack of the carboxy-terminus and was found in two patients, a boy and a girl of Turkish origin (*Table 1*), both with consanguineous parents

(first cousins). The boy developed a cystic fibrosis-like phenotype (125) located in the extracellular loop (*Figure 11D*) in the thumb (123). The truncated length of the protein is 204 amino acids and the approximate molecular weight is 28,58 kDa.

αR438fs

The deletion of a single base guanine in exon 8 (1311delG) of the α-subunit gene leads to a frameshift at position R438 which in turn leads to a premature stop codon (X43) in a Chinese patient (*Table 1*). The result is a loss of the carboxy-terminal domain (extracellular, helical and cytoplasmic). The girl had a heterozygous variation of the SCNN1A gene (126) located in the extracellular loop (*Figure 11E*) in the thumb (123). The truncated protein is 480 amino acids long and the approximately calculated molecular weight is 70,34 kDa.

γV543fs

The deletion of a guanin in exon 13* (1627delG) of the γ-subunit gene leads to a frameshift (γV543fs) in a Japanese patient (*Table 1*). The γV543fs mutation is located within the TM2 domain and is equivalent to αV563 (*Figure 11F*) (14). *Willam et al*. (14) determined, via sequence alignment with chicken ASIC1, that the position of the γV543fs mutation is eight residues away from the intracellular membrane at the lower part of the second transmembrane domain (TM2). This is in accordance with *Stockands et al*. (127) findings concerning the ENaC model. It results in a premature stop codon 166 nucleotides after and deletes the carboxy-terminus as well as most of the transmembrane spanning domain 2 (128). The truncated protein length is 597 amino acids and the approximate molecular weight is 81,04 kDa. Mutations that are found in the TM2 helix in hENaC subunits destroy the function of the subunit and, in this case, cause PHA1 (44).

* Location of mutation corrected by (107)

2 Aim of the study

The epithelial sodium channel is distributed among several tissues dependent on the subunits (2). ENaC in the kidney, an aldosterone targeted epithelium, is very important as ENaC in the distal nephron and the collecting duct is the crucial factor for the regulation of sodium and water homeostasis (1).

Mutations of ENaC subunits can lead to a gain or a loss of channel function and hence according to tissue type to different hereditary diseases (4–7). The lectin-like domain of TNF-α (TIP) is meant to enhance ENaC activity due to a higher open probability of the channel (9, 10) whereas the cell surface expression was just transiently increased (12). This TIP domain interacts with ENaC not only via N-glycosylation sites in the extracellular loop (96, 98) but also via the carboxy terminus (95, 122).

During my work on this thesis I observed ENaC frameshift mutants that have been reported to cause PHA1B and which lack the carboxy terminus. As the carboxy terminus has been reported being the site of interest (95) concerning the interaction of the TIP mimicking peptides AP301 and AP318 with ENaC, I investigated if the cell surface expression of mutant ENaCs was altered in presence of AP301 and AP318. More precisely, I studied if the channel function of loss-of-function phenotype of ENaC is restored by AP301 and AP318 as well due to an alternation in cell surface expression and not only because of the whole-cell current potentiating effect which has been reported by *Hazemi et al*. (11) and *Shabbir et al.* (12).

3 Materials and Methods

3.1 Cell culture

HEK-293 cells were used due to no endogenous expression of ENaC. The HEK-293 cells were seeded in a 75 cm^2 flasks in Dulbecco's modified Eagle medium/F12 nutrient mixture Ham plus L-glutamine (DMEM/F12), supplemented with 10 % fetal bovine serum (FBS) and 1 % penicillin-streptomycin (*Table 2*). Then they were stored in a humidified incubator at 37 °C with 5 % CO2 until they reached a confluence of 80–90 %. Afterwards the cells were split in to 11 100 mm cell culture dishes. Every step was carried out under the Laminar Air Flow.

TABLE 2. Cell culture reagents

Medium	Dulbecco's modified Eagle medium/F12 nutrient mixture Ham plus L-glutamine	500 ml
	Fetal bovine serum	50 ml
	Penicillin-streptomycin 1:1	5 ml
PBS without calcium and magnesium pH 7,4	NaCl	137 mM
	KCl	2,7 mM
	Na_2HPO_4	10 mM
	KH_2PO_4	0,5 mM
0,05 % Trypsin/EDTA	Trypsin/EDTA	

3.1.1 Transient transfection

After reaching a confluence of 80–90 %, the HEK-293 cells were transiently transfected with WT αβγ-hENaC or mutant (α- or γ-mutant)-ENaC and the complementing subunits (β and either α or γ) to form a complete channel. A transfection complex was prepared in an 1,5 ml microcentrifuge tube including serum free DMEM, X-tremeGENE™ HP DNA transfection reagent (*Table 3)* and DNA (*Table 4*) which was then incubated for 20 minutes at room temperature to form a complex. The medium was aspirated, then the cells were washed with 1X PBS and the transfection complex was added drop by drop to the cells. I prepared five dishes with WT DNA, five dishes with mutant-DNA and one dish with non-transfected HEK-

293 cells. Eventually, medium was added (DMEM + 10 % FBS + 1 % penicillin-streptomycin) and the cells were left in the incubator for transfection.

TABLE 3. Transfection reagents and DNA concentrations	
X-tremeGENE™ HP DNA Transfection Reagent	6 µl
Serum-free DMEM	150 µl
α-WT, αY447fs, αS243fs, αP197fs, αR438fs, γV543fs	600 ng
α-WT, β-WT, γ-WT (subunits to form a complete channel)	500 ng

TABLE 4. Concentration of utilized DNA	
α-hENaC WT	702,8 ng/µl
β-hENaC WT	771,3 ng/µl
γ-hENaC WT	659,2 ng/µl
αY447fs	619,0 ng/µl
αR438fs	758,3 ng/µl
αP197fs	710,3 ng/µl
αS243fs	717,7 ng/µl
γV543fs	648,1 ng/µl

3.1.2 Cell treatment with AP301 and AP318

After two to three days the transfection was highest and the cells were ready to be treated with AP301 and AP318 at a final concentration of 200 nM. After aspirating the medium, the cells were washed with ice-cold PBS and new medium was added. The cells were treated for 5 minutes respectively 10 minutes with each substance. Except one cell culture dish of wild-type, mutant and non-transfected HEK-293 cells were not treated with the substances.

3.2 Biotinylation

First, 5 ml of biotin solution (one vial EZ-Link® Sulfo-NH2-SS-Biotin in 55 ml ice-cold 1X PBS) were added to each cell culture dish. To cover all the cells with the biotin solution, they were incubated at 4 °C for 30 minutes with agitation. Then 200 µl quenching solution were added to each cell culture dish to stop the reaction and the cells were scraped and transferred to a 15 ml tube. All cell culture dishes were rinsed with 5 ml 1X PBS and the rinsed volume was added to the transferred cells. From then the proteins had to be stored on ice for the further steps. The cell suspension was centrifuged at 4000 x g for 1 minute at 4 °C and the supernatant was discarded. Then 200 µl of lysis buffer A (*Table 5*) were added, the cell pellet was resuspended and transferred into an 1,5 ml microcentrifuge tube. Then the cells were disrupted by ultrasonication (3 times for 10 seconds each). Eventually the cells were incubated on ice for 30 minutes. In the meantime the microcentrifuge tubes with 100 µl NeutrAvidin® Agarose beads solution were prepared. They were centrifuged at 1000 x g for 1 minute at 4 °C to collect the beads and washed with 100 µl Washing Buffer from the Biotinylation Kit and the supernatant was discarded. After 30 minutes the cell lysate was centrifuged at 14000 x g for 2 minutes by 4 °C to separate the intact cells and nuclei from the cell homogenate and the clarified supernatant was added to the NeutrAvidin® Agarose beads. The microcentrifuge tubes were incubated with agitation overnight at 4 °C.

The next day they were centrifuged for 5 minutes at 5000 x g and the supernatant was discarded. Then they were washed twice with 200 µl Washing Buffer A (*Table 5*), centrifuged and the supernatant was discarded again. To pull down the biotinylated proteins from the NeutrAvidin® Agarose beads 100 µl of 2X Sample buffer solution were added to each tube. The sample buffer contains β-mercaptoethanol to reduce the disulfide bonds for the cleavage of the spacer and protein unfolding, and bromophenol blue was added to trace the proteins in SDS-PAGE. Afterwards the eluates were denaturized at 65 °C for 10 minutes and then left on ice for 5 minutes. After the centrifugation the supernatant was transferred into a new tube and the gel pellet was discarded. Then the proteins were ready for analysis.

TABLE 5. Biotinylation reagents

Biotinylation Kit	EZ-Link® Sulfo-NHS-SS-Biotin (Sulfosuccinimidyl – 2-(biotinamido) ethyl-1,3-dithiopropionat)	
	Quenching solution	
	Lysis buffer	
	Immobilized NeutrAvidin® Gel	
	Washing buffer	
Lysis buffer A	Lysis buffer from biotinylation kit	4,5 ml
	0,2 M NaN_3 pH 5.5	10 ml
	4 % SDS	1 ml
	Protease inhibitor (leupeptin 10 mM or pepstatin A 10 mM)	50 µl
Washing buffer A	Washing buffer from biotinylation kit	2 ml
	Protease inhibitor	50 µ
4X SB	Glycerine	4 ml
	0,5 M TRIS HCl pH 6.8	4,8 ml
	SDS	0,8 g
	Bromophenol blue	4 mg
	β-mercaptothion	0,5 ml
	ddH_2O	0,7 ml
2X SB	4X SB	600 µl
	ddH_2O	600 µl
	protease inhibitor E-64	15 µl
1X SB	4X SB	150 µl
	ddH_2O	450 µl
	Protease inhibitor E-64	7,5 µl

Biotinylation is a cell surface treatment which benefits from the high binding affinity – the strongest non-covalent interaction – of biotin (vitamin B7/H) with avidin. You can isolate surface proteins with this method and study the expression or the trafficking of surface molecules Biotin is not able to pass through intact cell membranes therefore it is attached to the cell surface ENaCs (129). I used NeutrAvidin®, a deglycosylated form of avidin (the latter

has the same binding affinity for biotin as streptavidin) because of its lower nonspecific binding property due to a lack of glycoproteins (130). In my case the ENaC proteins on the cell surface were biotinylated as the charged Sulfosuccinimidyl (Sulfo-NHS) ester of biotin is not capable of overcoming the cell membrane barrier *(Figure 12)*. The Sulfo-NHS group (reactive group) modifies primary amino groups in the protein as it acts as a nucleophile and forms a bond with lysines located in the sidechains of the protein. The biotinylated ENaC proteins bind the NeutrAvidin® Agarose beads and due to a cleavable spacer (SS) and they can be isolated through hydrolytic splitting of the disulfide bridge (131) *(Figure 13)*.

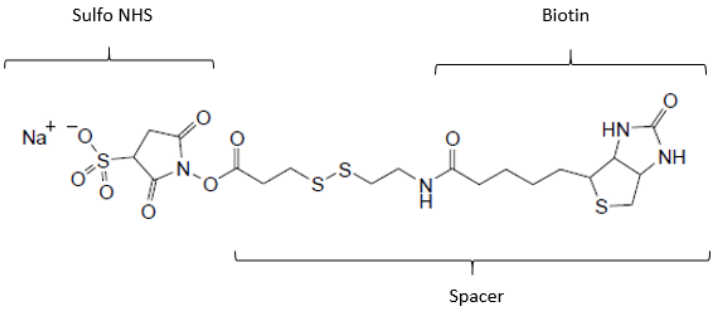

***FIGURE 12*. Chemical structure of Sulfo-NHS-SS-Biotin.**

(Source*:* figure from http://www.uab.edu/proteomics/bmsf/educationprotocols/protocols/CSPI.pdf, modified*)*

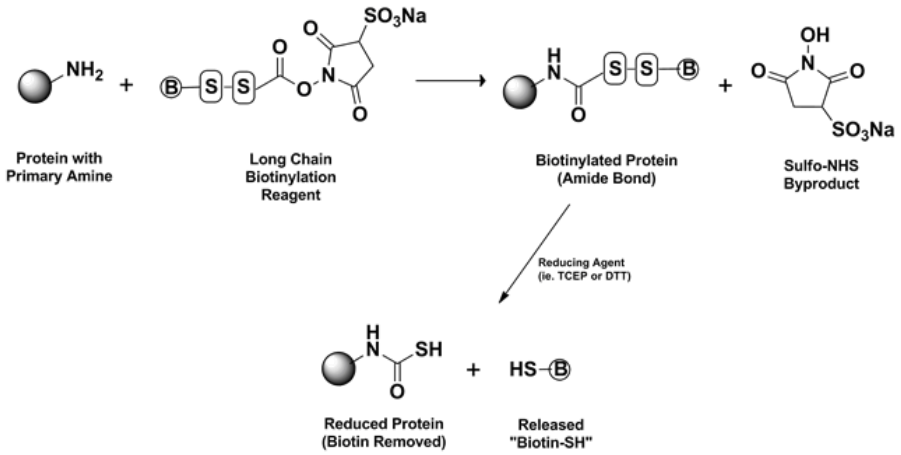

***FIGURE 13*. Scheme of protein biotinylation with Sulfo-NHS-SS-Biotin.**

(Source: figure from https://www.covachem.com/sulfo_nhs_ss_biotin.html)

3.3 Western blot

3.3.1 Electrophoresis

Then the proteins were separated under reducing conditions based on their molecular weight by SDS-PAGE. Corresponding amounts of proteins along with a color-coded prestained protein marker (High Range, 43–315 kDa) were applied to the gel after it had been passed over into the electrophoresis basin filled with 1X running buffer (*Table 7*). The proteins accumulated in a 4 % stacking gel (*Table 6*) to obtain sharp bands and were separated in a 7,5 % separating gel (*Table 6*). As the result of the anionic detergent SDS, the proteins were denaturized and their intrinsic charge was covered. The electrophoresis run at 200 V for about 40 minutes. For each mutant three Western blots were performed.

TABLE 6. Composition of gels

7,5 % separating gel	ddH_2O	2,91 ml
	30 % acrylamide	1,5 ml
	1,5 M TRIS HCl pH 8,8	1,5 ml
	10 % SDS	60 µl
	10 % APS	30 µl
	TEMED	3 µl
4 % stacking gel	ddH_2O	2,24 ml
	30 % acrylamide	0,5 ml
	1,5 M TRIS HCl pH 8,8	0,945 ml
	10 % SDS	37,5 µl
	10 % APS	37,5 µl
	TEMED	3,8 µl

3.3.2 Semi-dry blotting

After their separation the proteins were transferred from the gel onto a nitrocellulose membrane (UltraCruz™ 0.45 mm, Santa Cruz Biotechnology, Texas, USA). The separating gel, a nitrocellulose-membrane and two filter papers were first drained in 1X towbin buffer (*Table 7*) and then transferred to the blotting cassette which was inserted in the Trans-Blot® Turbo™ Transfer System (Bio Rad Laboratories, Vienna, Austria). The proteins were transferred from gel to membrane at 25 V for 30 minutes to be partially renatured.

TABLE 7. Composition of buffers

10X running buffer	TRIS Base	30 g
	Glycine	144 g
	SDS	10 g
	ddH_2O	ad 1 l
1X running buffer	10X running buffer	100 ml
	ddH_2O	900 ml
5X towbin buffer	TRIS Base	25 mM → 15,14 g
	Glycine	192 mM → 72,07 g
	SDS	0,1 % → 5 g
	Methanol	20 % → 1 l
	Mouble-distilled water	ad 5 l

3.3.3 Immunoblotting

To block non-specific binding sites the membrane was incubated with a blocking solution *(Table 8)* at 4 °C for 90 minutes or overnight under agitation. The primary antibody (AB) was a polyclonal AB which recognizes several epitopes of ENaC (α or γ) and therefore has a higher binding affinity. Prior to that, it is necessary to block unoccupied sites so that the antibody only binds the demanded protein. After washing the membrane once with 1X PBST, the primary antibody solution was added, followed by an incubation for at least 90 minutes. After washing the membrane five times with 1X PBST, the secondary antibody solution was added. The horseradish-peroxidase (HRP) linked monoclonal secondary antibody binds specifically the primary AB and was used to amplify the signal. After an incubation time of at least 90 minutes, the secondary AB solution was discarded and the membranes were cleaned by washing three times with 1X PBST and then once with 1X PBS to remove the detergent. The primary antibody solution contained NaN_3 to prevent it from contamination, whereas the secondary antibody solution must not contain NaN_3, otherwise it would inactivate the HRP.

TABLE 8. Composition of reagents for immunoblotting

Blocking solution	3 % BSA (bovine serum albumin)	1,5 g
	0,2 % NaN_3	100 µl
	PBS	50 ml
10X PBS	NaCl	80 g
	KCl	2 g
	Na_2HPO_4	14,4 g
	KH_2PO_4	2,4 g
1X PBS	10X PBS	100 ml
	ddH_2O	ad 1 l
1X PBST	1X PBS	1 l
	Tween 20	1 ml

TABLE 9. Antibodies for immunoblotting

ANTIBODY	*DILUTION*	*MOLECULAR WEIGHT*
anti-α-EnaC from goat	1:1000	80–110 kDa
anti-goat IgG, HRP-linked from donkey	1:3000	
anti-α-EnaC from rabbit	1:1000	80–110 kDa
anti-rabbit IgG, HRP-linked from goat	1:3000	
anti-γ-EnaC from goat	1:1000	85–95 kDa
anti-β-Tubulin from mouse	1:3000	55 kDa
anti-mouse IgG, HRP-linked from goat	1:10000	

3.3.4 Detection and Evaluation

Proteins were visualized with ECL (enhanced chemiluminescence) substrate (1 ml detection reagent 1 + 1 ml detection reagent 2). After the incubation of the membranes for two to three minutes the detection was carried out in the dark room. Since the HRP oxidates the substrate (luminol) which returns to its ground state by emitting light, the expected proteins can be visualized by exposing the membranes to the X-ray films (Amersham Hyperfilm ECL, GE Healthcare).

Immunoblotting and detection were performed on the same principle for the loading control tubulin which is necessary to prove that the samples were loaded in comparable amounts and whether the transfer from gel to membrane worked or not.

Image Studio Lite was used for quantification and Microsoft Excel was used for chart generation and for calculations. Statistical analysis was performed with Excel and GraphPad and statistical significance was set at $p < 0,05$ (*$p < 0,05$ significant, **$p < 0,01$ highly significant and ***$p < 0,001$ extremely significant). Data are represented as mean ± SEM of three independent replicants for *αY447fs, αS243fs, αP197fs*, *αR438fs*, *γV543fs* and *WT γ(αβ)-ENaC* and nine different replicants for *WT α(βγ)-ENaC*. Significant differences were determined by unpaired t-test.

A list of used drugs and chemical reagents has been attached (*Appendix_9.3.Used drugs/chemical reagents and their providers*).

4 Results

In my experiments I used HEK-293 cells to study the effect of AP301 and AP318 on the cell surface expression of α- and γ-ENaC and some of their mutants. All the examined frameshift mutations lead to a premature stop codon which results in the lack of the carboxy-terminal domain. This domain has been reported to be one site of interaction (95) (as well as N-glycan moieties in the extracellular loop (12)) of the lectin-like domain (TIP) of TNF with the α-subunit of the epithelial sodium channel.

William et al. (13, 14) showed a significant decrease of the amiloride-sensitive sodium current of the mutants αY447fs (13), αP197fs (13), αR438fs (13), αS243fs (14) and γV543fs (14) compared to the respective WT. Although these mutants lack the carboxy terminus, solnatide led to increased currents compared to mutant control (without solnatide) and WT control (13, 14). AP318 as well had a current potentiating effect on αS243fs and γV543fs mutant (14).

I investigated the alternation in the cell surface expression of WT α- and γ-hENaC and the above mentioned mutants lacking the carboxy terminus after the treatment with AP301 and AP318. The α-mutants were co-transfected with WT βγ-ENaC whereas the γV543 frameshift mutant was co-transfected with WT αβ-ENaC. The cells were treated with a concentration of 200 nM AP301 and AP318 which has been reported to be the concentration inducing the maximal current-enhancing effect in ENaC (11). Whereas the effect on the amiloride-sensitive sodium current was consistent (13, 14), the cell surface abundance varied without and after the treatment with AP301 and AP318. The expression of the untreated mutants was compared to their respective WT control (=1), whereas the expression of the treated mutants was compared to the respective non-treated mutant control.

4.1 Effect of AP301 and AP318 on cell surface expression of WT α(βγ)-hENaC

For a better understanding on how AP301 (INN: solnatide) and AP318 affect α-frameshift mutations, I examined their influence on WT α(βγ)-ENaC as well. Therefore HEK-293 cells were transiently transfected with a complex of WT α(βγ)-hENaC. They do not express ENaC endogenously (132) hence non-transfected HEK-293 cells were used as a negative control. The transfected HEK-293 cells were treated in a time-dependent manner (5 or 10 minutes) with 200 nM AP301 and AP318 and one cell culture plate was left untreated. After the biotinylation the proteins were separated under reducing conditions by SDS-PAGE and transferred onto a

nitrocellulose membrane by semi-dry blotting. Immunoblotting was carried out to detect the target protein. Concerning this experiment, the untreated WT α(βγ)-hENaC (positive control) was shown in relation with the treated WT α(βγ)-hENaC. Moreover, the untreated WT α(βγ)-ENaC was used as reference for all the other untreated frameshift mutants to show the relation.

After the treatment with AP301 for 5 minutes the increase in the cell surface expression of WT α(βγ)-ENaC was statistically significant (1,48 ± 0,23, n=12) compared to the untreated WT α(βγ)-ENaC. Even though the expression was lower after 10 minutes with AP301, there was still a statistically significant increase (1,25 ± 0,12, n=12) compared to the expression of the untreated WT α(βγ). The cell surface expression in presence of AP318 was not as much increased as with AP301. However, after a 5-minute treatment with AP318 the expression was increased about 1,21-fold ± 0,16 (n=12) and after a 10-minute treatment with AP318 the difference was not significant (1,05 ± 0,40, n=12) anymore (*Figure 14*).

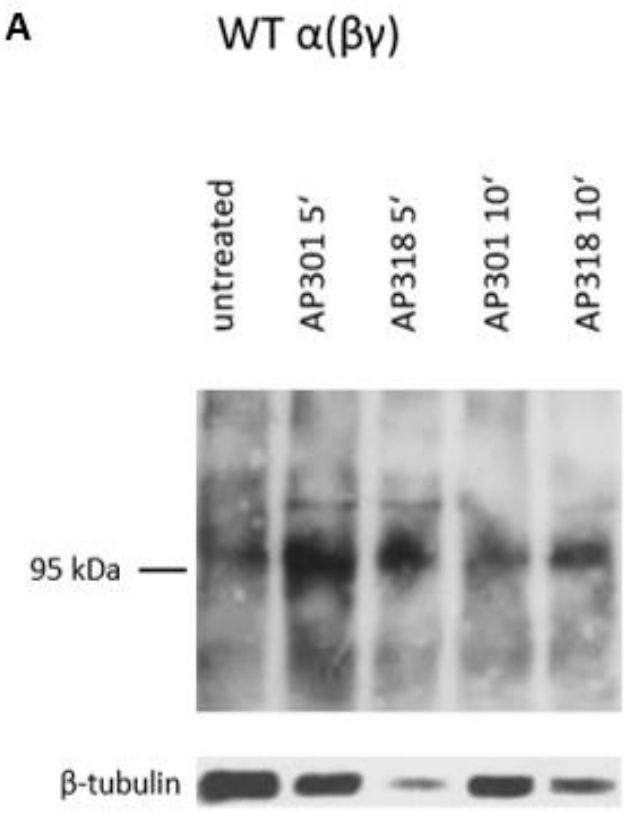

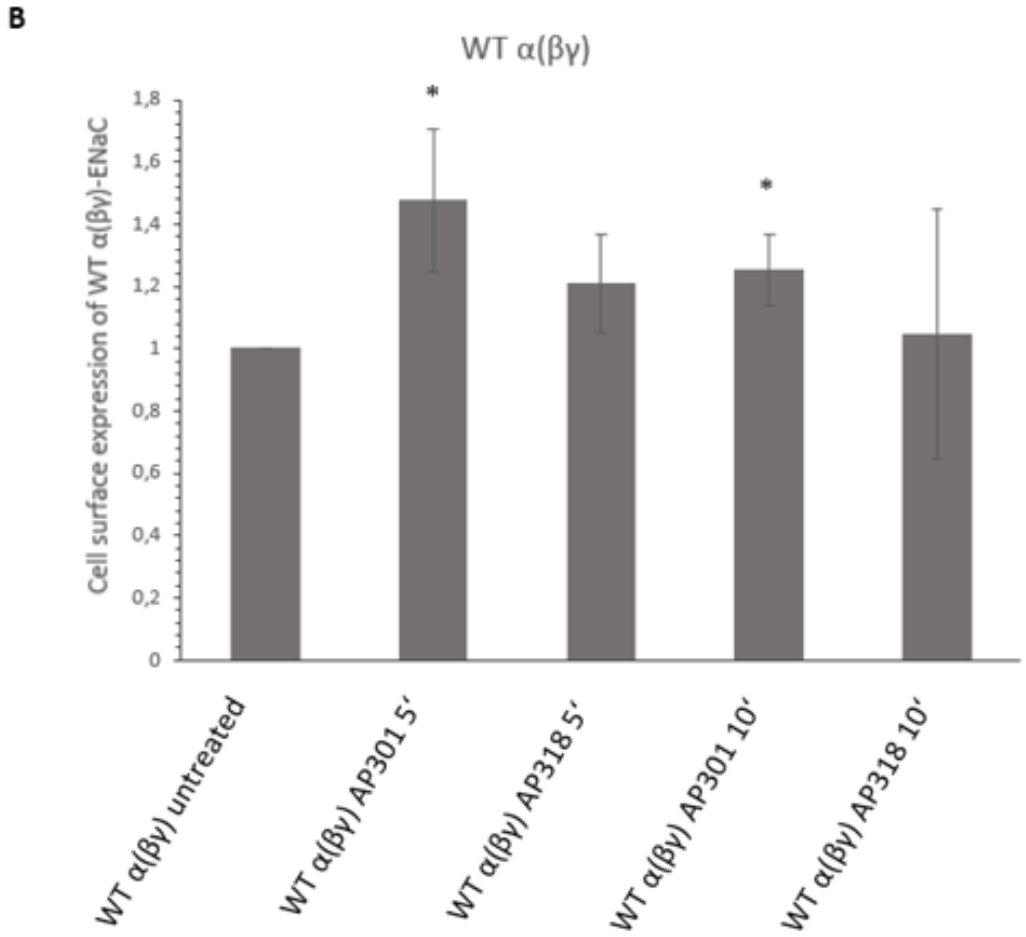

FIGURE 14. **Results for WT α(βγ)-hENaC after time-dependent treatment with AP301 and AP318.**

(A) Effect on membrane abundance of WT α(βγ)-hENaC after time-dependent treatment with AP301 and AP318 in transiently transfected HEK-293 cells.

A complex of WT α(βγ)-ENaC was heterologously expressed in HEK-293 cells. Cells were treated with 200nM AP301 and AP318 for 5 and 10 minutes each or untreated (control). After separation by SDS-PAGE, the biotinylated surface proteins were visualized with anti-α-ENaC antibodies. WT α-ENaC shows a band at about 95 kDA, whereas β-tubulin shows a band at about 55 kDa. β-tubulin was used as loading control for relative quantification of the expression of WT α(βγ)-ENaC. Twelve blots were performed using independent biological replicants and one representative is shown.

(B) Densiometric analysis of WT α(βγ)-hENaC expression.

WT α(βγ) untreated was used as control (=1). WT α(βγ)-ENaC was treated with 200 nM AP301 or AP318 for 5 or 10 minutes. The expression of WT α(βγ)-ENaC was normalized compared to β-tubulin and set in relation to WT α(βγ) control. Results are shown as mean ± SEM. Significant differences are indicated, * $p<0,05$ (n=12).

4.2 Effect of AP301 and AP318 on cell surface expression of mutant αY447fs

Untreated WT α(βγ)-ENaC was used as reference (=1) for untreated αY447fs(βγ) mutant. The expression of untreated αY447fs(βγ) mutant was almost the same as untreated WT α(βγ) (1,07 ± 0,13, n=3). After the treatment with AP301 for 5 minutes and 10 minutes the increase in the cell surface expression of both was significantly higher compared to control whereby the expression after the treatment with AP301 for 10 minutes (1,57 ± 0,12, n=3) was higher than after the treatment with AP301 for 5 minutes (1,46 ± 0,05, n=3). The cell surface expression after the 5-minute treatment with AP318 showed an increase of about 1,52-fold ± 0,15 (n=3). Although the cell surface expression was still increased after a 10-minute treatment with AP318, the difference was not significant (1,42 ± 0,28, n=3) anymore (*Figure 15*).

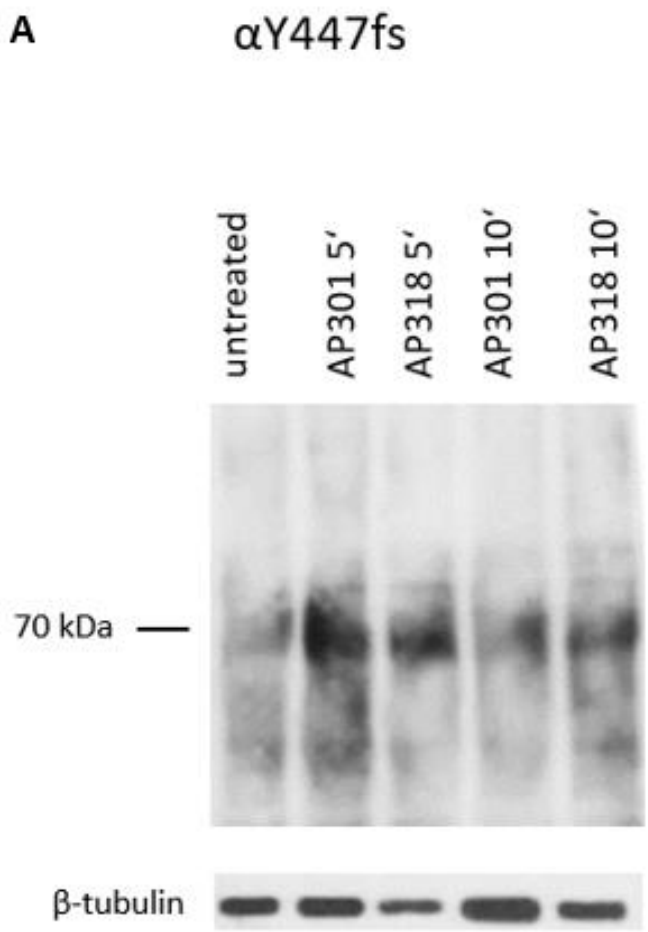

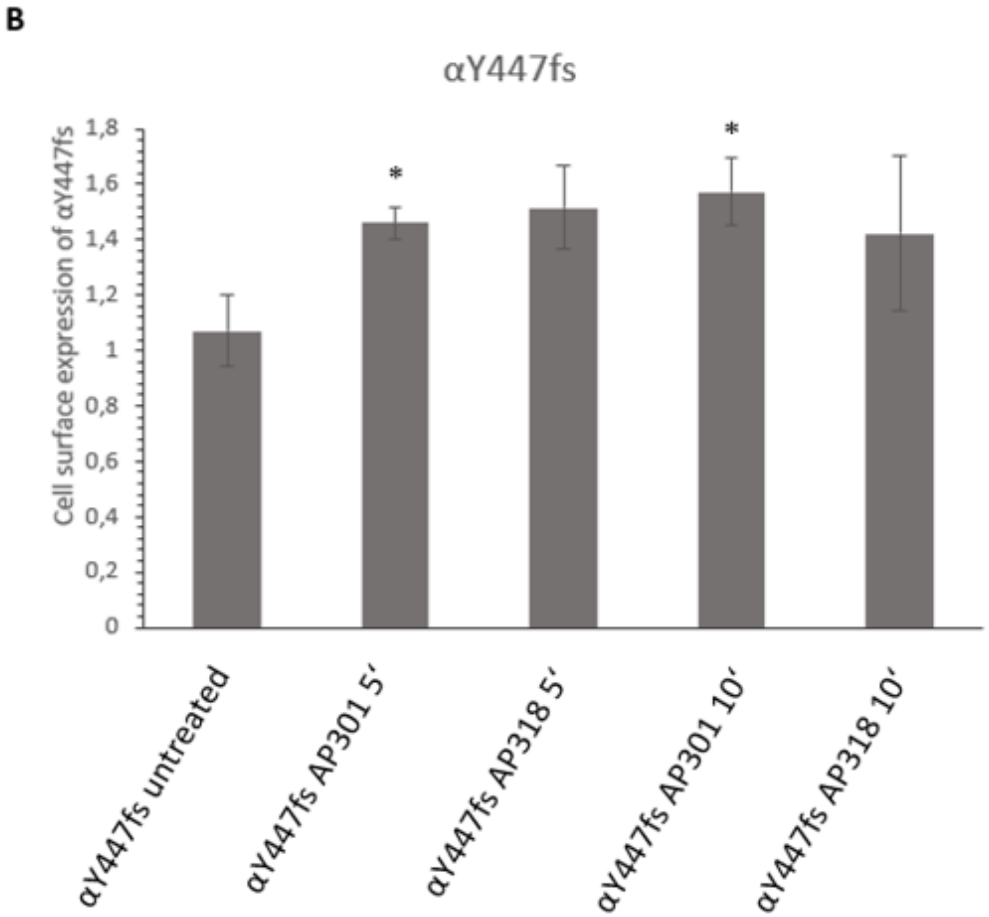

FIGURE 15. **Results for αY447fs(βγ)-hENaC after time-dependent treatment with AP301 and AP318.**

(A) Effect on membrane abundance of αY447fs(βγ)-hENaC after time-dependent treatment with AP301 and AP318 in transiently transfected HEK-293 cells.

A DNA complex of the mutant αY447fs and WT (βγ) was heterologously expressed in HEK-293 cells. Cells were treated with 200 nM AP301 and AP318 for 5 and 10 minutes each or untreated (control). After separation under reducing conditions by SDS-PAGE the biotinylated surface proteins were blotted semi-dry and visualized by immunoblotting with anti α-ENaC antibodies. The truncated mutant is shorter than WT α(βγ)-ENaC (95 kDa) and the line indicates the relevant band. β-tubulin shows a band at about 55 kDa and was used as loading control for relative quantification of the expression of αY447fs(βγ)-ENaC. Three blots were performed using independent biological replicants and one representative is shown.

(B) Densiometric analysis of αY447fs(βγ)-hENaC expression.

αY447fs(βγ)-ENaC was treated with 200 nM AP301 or AP318 for 5 or 10 minutes or untreated. The expression of αY447fs(βγ)-ENaC was normalized compared to β-tubulin and set in relation to the untreated control. Results are shown as mean ± SEM. Significant differences are indicated, *$p < 0,05$ (n=3).

4.3 Effect of AP301 and AP318 on cell surface expression of mutant αS243fs

The cell surface expression was increased without a treatment and even more with AP301 and AP318. Untreated αS243fs(βγ) (control) had a 2,31-fold ± 0,17 (n=3) increase in the cell surface expression compared to untreated WT α(βγ) , which was extremely significant. After the treatment with AP301 for 5 minutes the cell surface expression was extremely increased about 4,33-fold ± 0,12 (n=3) and after 10 minutes the increase was still significant (3,41 ± 0,29, n=3). The expression after the 5-minute treatment with AP318 was highly increased (4,10 ± 0,33, n=3)) and even if the expression was not as high after the 10-minute treatment with AP318 (3,84 ± 0,10, n=3) as it was after the 5-minute treatment, the increase in the cell surface expression was still highly significant. In conclusion, the expression after the treatment with AP301 and AP318 for 5 minutes was very much increased compared to the untreated control. Although a decrease was shown after being treated for 10 minutes with the two substances, the cell surface abundance was still a lot higher compared to the control (*Figure* 16).

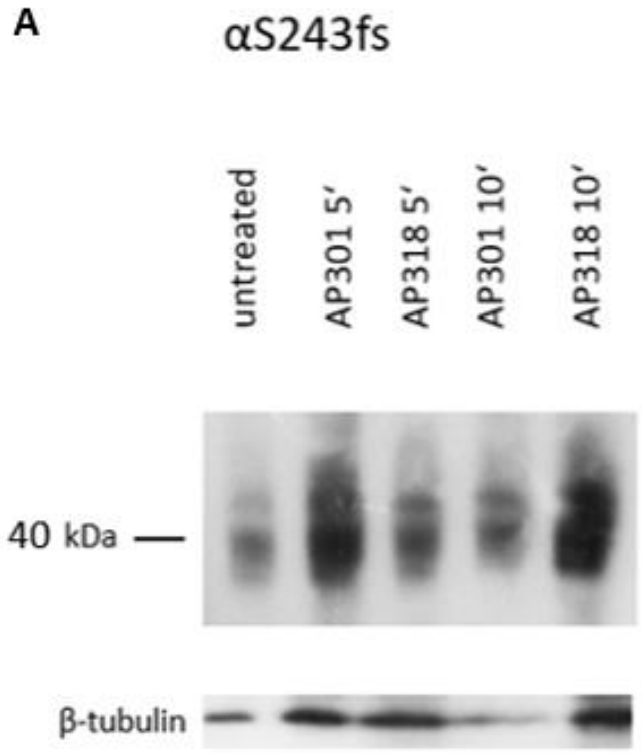

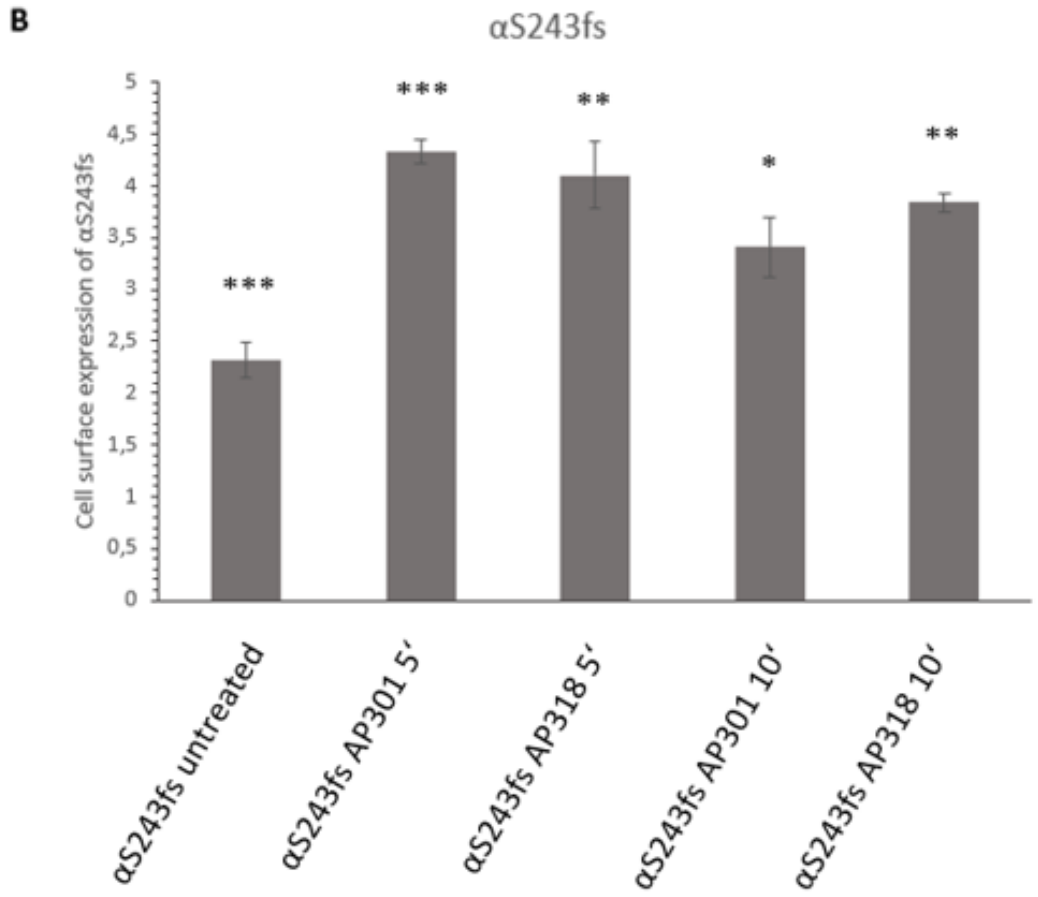

FIGURE 16. **Results for αS243fs(βγ)-hENaC after time-dependent treatment with AP301 and AP318.**

(A) Effect on membrane abundance of αS243fs(βγ)-hENaC *after time-dependent treatment with AP301 and AP318 in transiently transfected HEK-293 cells.*

αS243fs was co-expressed with WT (βγ)-ENaC in HEK-293 cells. Cells were treated with 200 nM AP301 and AP318 for 5 and 10 minutes each or untreated (control). After separation under reducing conditions by SDS-PAGE the biotinylated surface proteins were transferred onto a membrane by tank blotting and visualized by immunoblotting with anti α-ENaC antibodies. The truncated mutant is shorter than WT α(βγ)-ENaC (95 kDa) and the line indicates the relevant band. β-tubulin shows a band at about 55 kDa and was used as loading control for relative quantification of the expression of αS243fs(βγ)-ENaC. Three blots were performed using independent biological replicants and one representative is shown.

(B) Densiometric analysis of αS243fs(βγ)-hENaC expression.

αS243fs(βγ)-ENaC was treated with 200 nM AP301 or AP318 for 5 or 10 minutes or untreated. The expression of αS243fs(βγ)-ENaC was normalized compared to β-tubulin and set in relation to the untreated control. Results are shown as mean ± SEM. Significant differences are indicated, *$p < 0,05$, **$p < 0,01$ and *** $p < 0,001$ (n=3).

4.4 Effect of AP301 and AP318 on cell surface expression of mutant αP197fs

The untreated αP197fs(βγ) mutation (control) showed a slight increase in the cell surface expression compared to WT α(βγ) control of about 1,16-fold ± 0,04 (n=3), which was extremely significant. Although the 1,63-fold ± 0,10 (n=3) increase in the cell surface abundance of αP197fs(βγ) was significant after a 5-minute treatment with AP301, I also observed a significant decrease after the 10-minute treatment with AP301 of about the half (0,50 ± 0,17, n=3) of the cell surface expression compared to untreated mutant control. Therefore, I conclude that with AP301 only the translocation of αP197fs(βγ) to the cell membrane and not the expression was increased. With AP318 I observed an increase in cell surface abundance after 5 minutes (1,12 ± 0,28) which was even higher after 10 minutes (1,26 ± 0,07) but both values were not statistically significant (*Figure 17*).

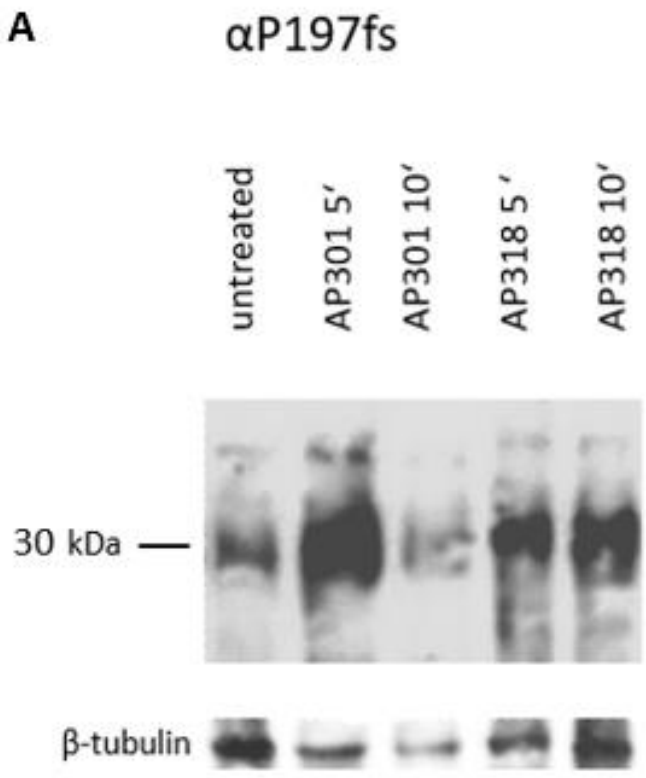

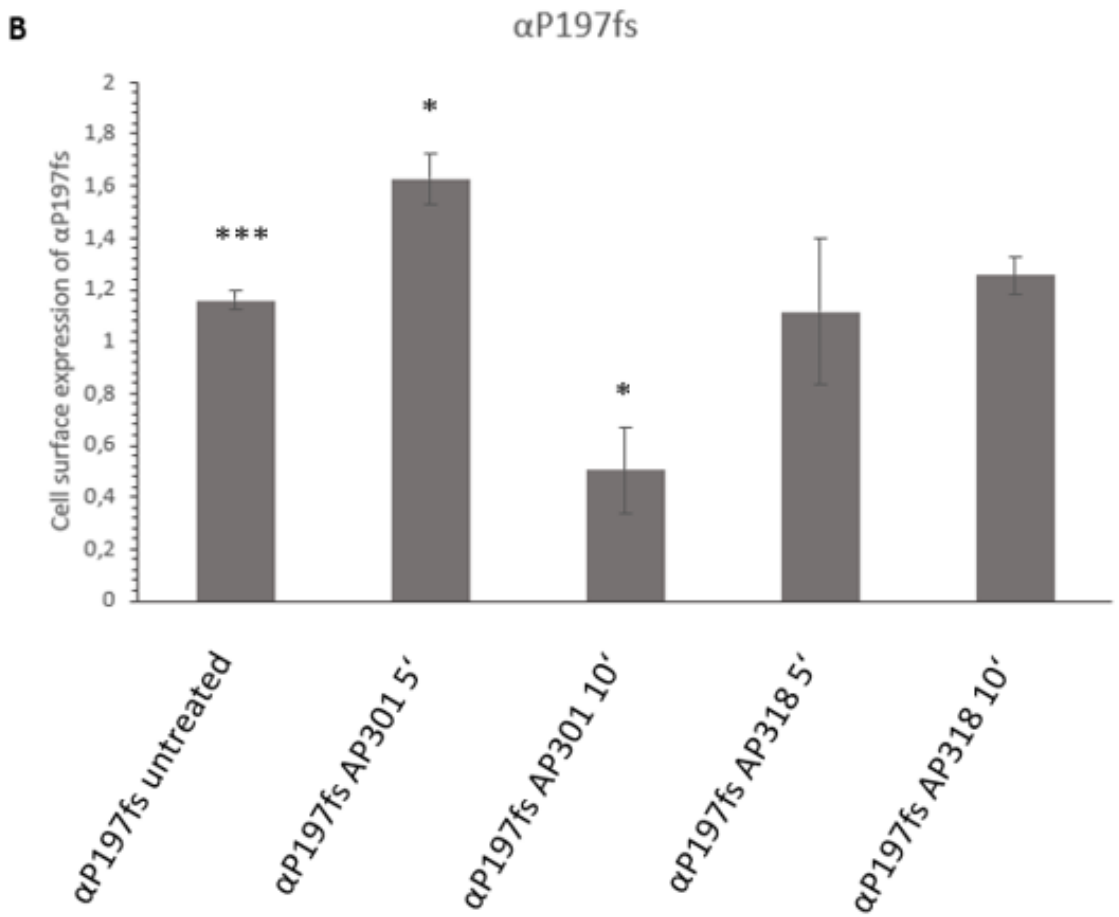

FIGURE 17. **Results for αP197fs(βγ)-hENaC after time-dependent treatment with AP301 and AP318.**

(A) Effect on membrane abundance of αP197fs(βγ)-hENaC *after time-dependent treatment with AP301 and AP318 in transiently transfected HEK-293 cells.*

αP197fs was co-expressed with WT (βγ)-ENaC in HEK-293 cells. Cells were treated with 200 nM AP301 and AP318 for 5 and 10 minutes each or untreated (control). After separation under reducing conditions by SDS-PAGE the biotinylated surface proteins were blotted semi-dry and visualized by immunoblotting with anti α-ENaC antibodies. The truncated mutant is shorter than WT α(βγ)-ENaC (95 kDa) and the line indicates the relevant band. β-tubulin shows a band at about 55 kDa and was used as loading control for relative quantification of the expression of αP197fs(βγ)-ENaC. Three blots were performed using independent biological replicants and one representative is shown.

(B) Densiometric analysis of αP197fs(βγ)-hENaC expression.

αP197fs(βγ)-ENaC was treated with 200 nM AP301 or AP318 for 5 or 10 minutes or untreated (control). The expression of αP197fs(βγ)-ENaC was normalized compared to β-tubulin and set in relation to the control. Results are shown as mean ± SEM. Significant differences are indicated, *$p < 0,05$ and ***$p < 0,001$ (n=3).

4.5 Effect of AP301 and AP318 on cell surface expression of mutant αR438fs

The untreated αR438fs(βγ) mutant (control) only had an 1,09-fold ± 0,08 (n=3) increase in the cell surface abundance compared to WT α(βγ)-ENaC control, which nevertheless was statistically significant. Solnatide (AP301) even decreased the cell surface abundance of this αR438 frameshift mutant after 5 and 10 minutes to a lower level than the control. The decrease after 5 minutes with solnatide (0,73 ± 0,10, n=3) was statistically significant but after 10 minutes (0,86 ±0,22, n=3) no statistical significance was indicated anymore. The AP318 treatment showed an increased cell surface expression after 5 minutes (1,65 ± 0,34, n=3) and 10 minutes compared to the control whereby only after 10 minutes with AP318 (1,46 ± 0,07, n=3) the expression was significant. (*Figure 18*).

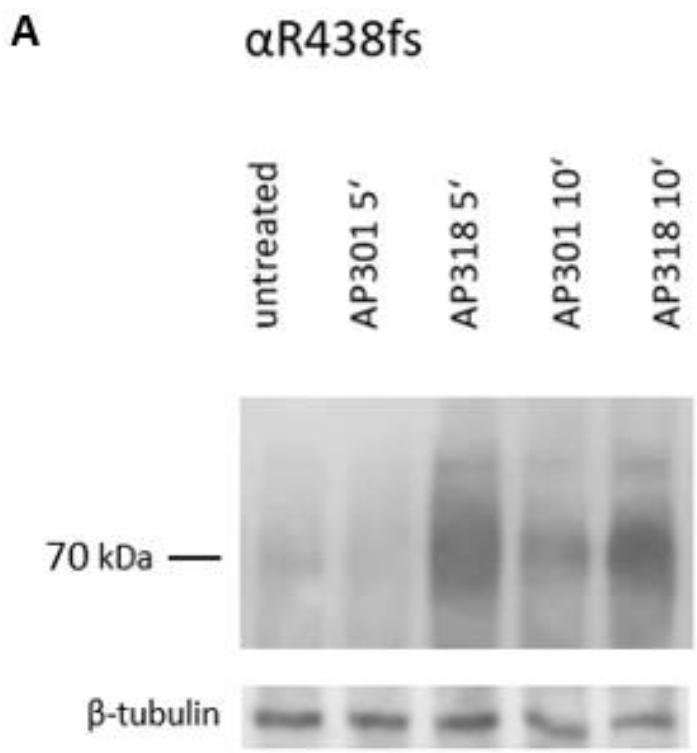

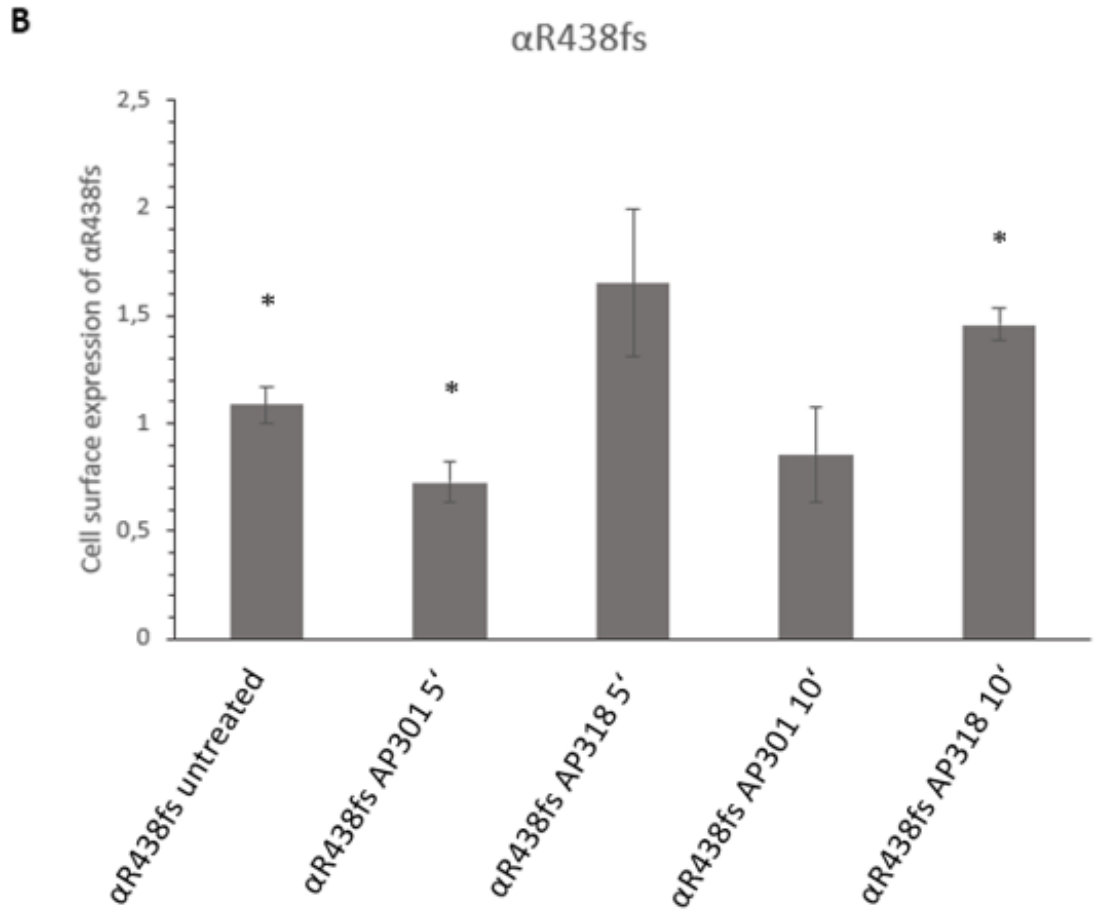

FIGURE 18. **Results for αR438fs(βγ)-hENaC after time-dependent treatment with AP301 and AP318.**

(A) Effect on membrane abundance of αR438fs(βγ)-hENaC after time-dependent treatment with AP301 and AP318 in transiently transfected HEK-293 cells.

αR438fs was co-expressed with WT (βγ)-ENaC in HEK-293 cells. Cells were treated with 200 nM AP301 and AP318 for 5 and 10 minutes each or untreated (control). After separation under reducing conditions by SDS-PAGE the biotinylated surface proteins were blotted semi-dry and visualized by immunoblotting with anti α-ENaC antibodies. The truncated mutant is shorter than WT α(βγ)-ENaC (95 kDa) and the line indicates the relevant band. β-tubulin shows a band at about 55 kDa and was used as loading control for relative quantification of the expression of αR438fs(βγ)-ENaC. Three blots were performed using independent biological replicants and one representative is shown.

(B) Densiometric analysis of αR438fs(βγ)-hENaC expression.

αR438fs (βγ)-ENaC was treated with 200 nM AP301 or AP318 for 5 or 10 minutes or untreated (control). The expression of αR438fs(βγ)-ENaC was normalized compared to β-tubulin and set in relation to WT control. Results are shown as mean ± SEM. Significant differences are indicated, *$p < 0,05$ (n=3).

4.6 Effect of AP301 and AP318 on cell surface expression of WT γ(αβ)-hENaC

I did not only observe the effect of AP318 and AP301 on the cell surface abundance of α-frameshift mutations, but also of a frameshift mutation in the γ-subunit. This experiment was realized in an analogous manner as above but with a heterologous transfection of HEK-293 cells with a WT γ(αβ)-ENaC complex. The results presented in *Figure 19* show that solnatide (AP301) and AP318 did not alter the cell surface expression in a significant way. After the treatment with AP301 for 5 minutes I observed a decrease (0,87 ± 0,08, n=3) in the cell surface expression compared to untreated WT γ(αβ) (control). A slight increase of 1,08-fold ± 0,08 (n=3) followed the 10-minute treatment with AP301. The cell surface abundance in presence of AP318 was more increased than with AP301. After 10 minutes with AP318 (1,23 ± 0,10, n=3) the increase was higher than after 5 minutes with AP318 (1,14 ± 0,13, n=3).

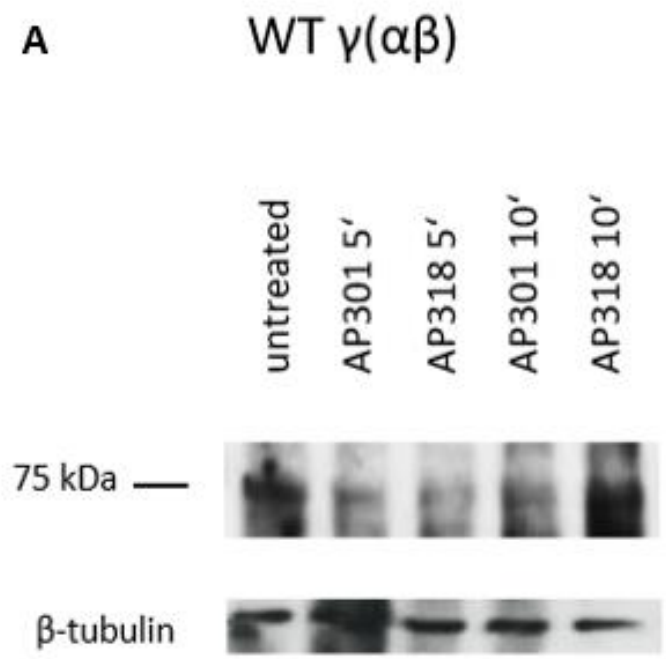

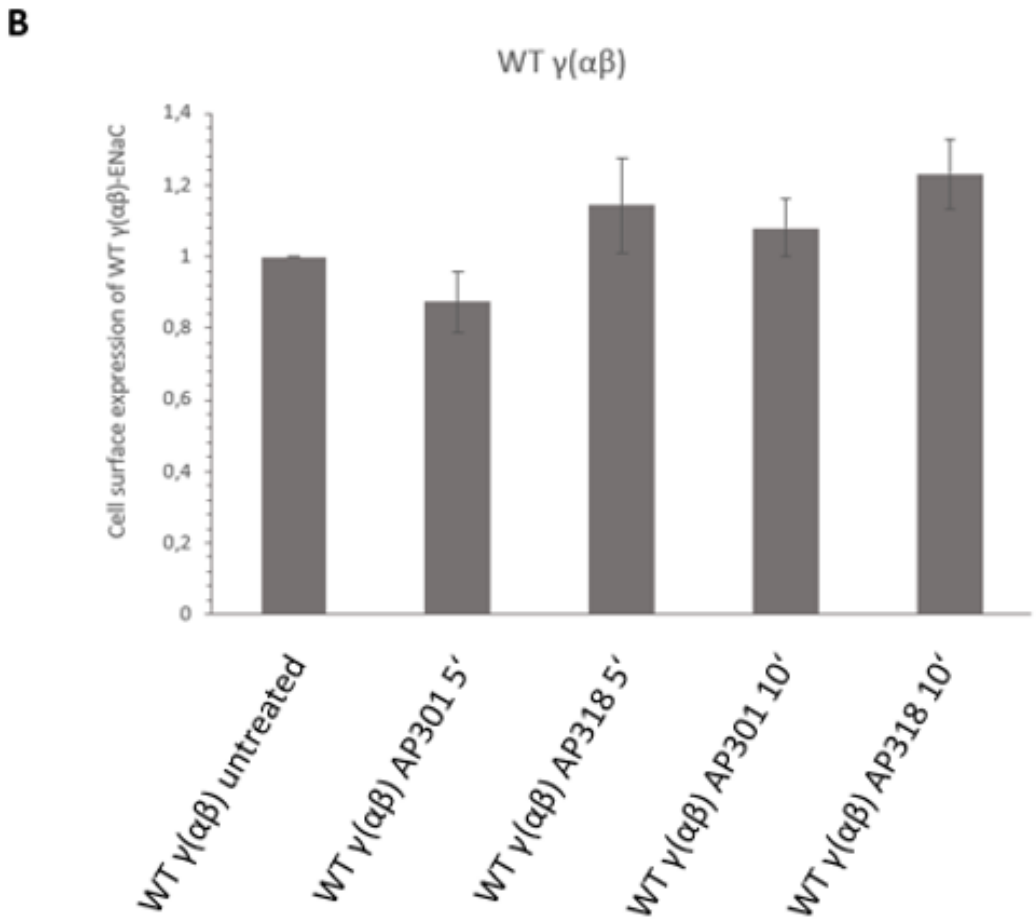

FIGURE 19. **Results for WT γ(αβ)-hENaC after time-dependent treatment with AP301 and AP318.**

(A) Effect on membrane abundance of WT γ(αβ)-hENaC after time-dependent treatment with AP301 and AP318 in transiently transfected HEK-293 cells.

Cells were treated with 200 nM AP301 and AP318 for 5 and 10 minutes each or untreated (control). After separation by SDS-PAGE, the biotinylated surface proteins were visualized with anti-γ-ENaC antibodies. WT γ-ENaC shows a band at about 75 kDA, whereas β-tubulin shows a band at about 55 kDa. β-tubulin was used as loading control for relative quantification of the expression of WT γ(αβ)-ENaC. Three blots were performed using independent biological replicants and one representative is shown.

(B) Densiometric analysis of WT γ(αβ)-hENaC expression.

The untreated WT γ(αβ) was used as control (=1). WT γ(αβ)-ENaC was treated with 200 nM AP301 or AP318 for 5 or 10 minutes was set in relation to WT control. The expression of WT γ(αβ)-ENaC was normalized compared to β-tubulin and set in relation to WT γ(αβ) control. Results are shown as mean ± SEM. There was no significant increase in cell surface expression of WT γ(αβ) after treatment with AP301 and AP318, (n=3).

4.7 **Effect of AP301 and AP318 on cell surface expression of mutant γV543fs**

I observed a highly significant increase in cell surface abundance after the 5-minute treatment with AP301 and a statistically significant increase after the 10-minute treatment with AP301. Nevertheless, the cell surface abundance was lower after 10 minutes (1,17 ± 0,04, n=3) than after 5 minutes (1,44 ± 0,06, n=3) with AP301. Hence I can deduce that the higher cell surface abundance was not because of a higher level of expression but of translocation of the γV543fs(βγ) mutant. The untreated mutant (control) showed a decrease in cell surface expression lower than WT γ(αβ) control (0,79 ± 0,09, n=3) and the expression level with AP318 was even lower than the mutant control level. There was a 0,65-fold ± 0,13 (n=3) decrease of the cell surface abundance after 5 minutes with AP318 and an even higher decrease after 10 minutes (0,54 ± 0,06, n=3). Concerning this mutant AP301 and AP318 led to a higher translocation rate and not to a higher cell surface expression as the cell surface abundance decreases after 10 minutes compared with the 5-minute treatment (*Figure 20).*

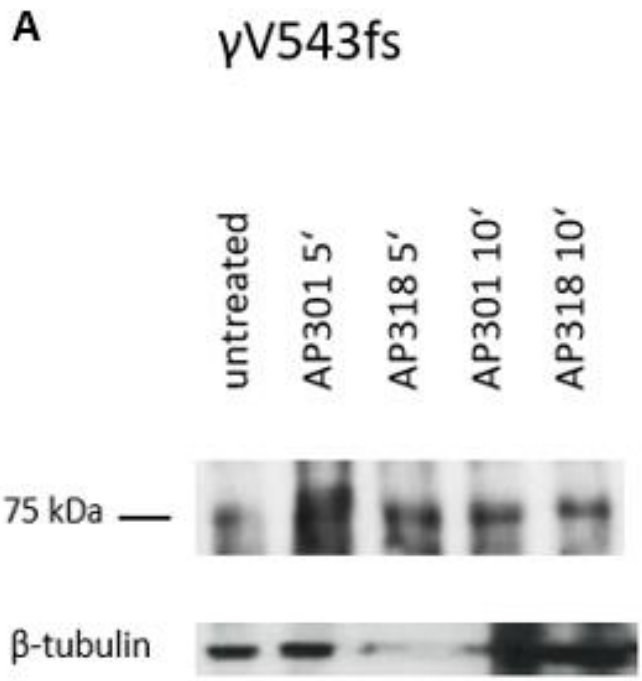

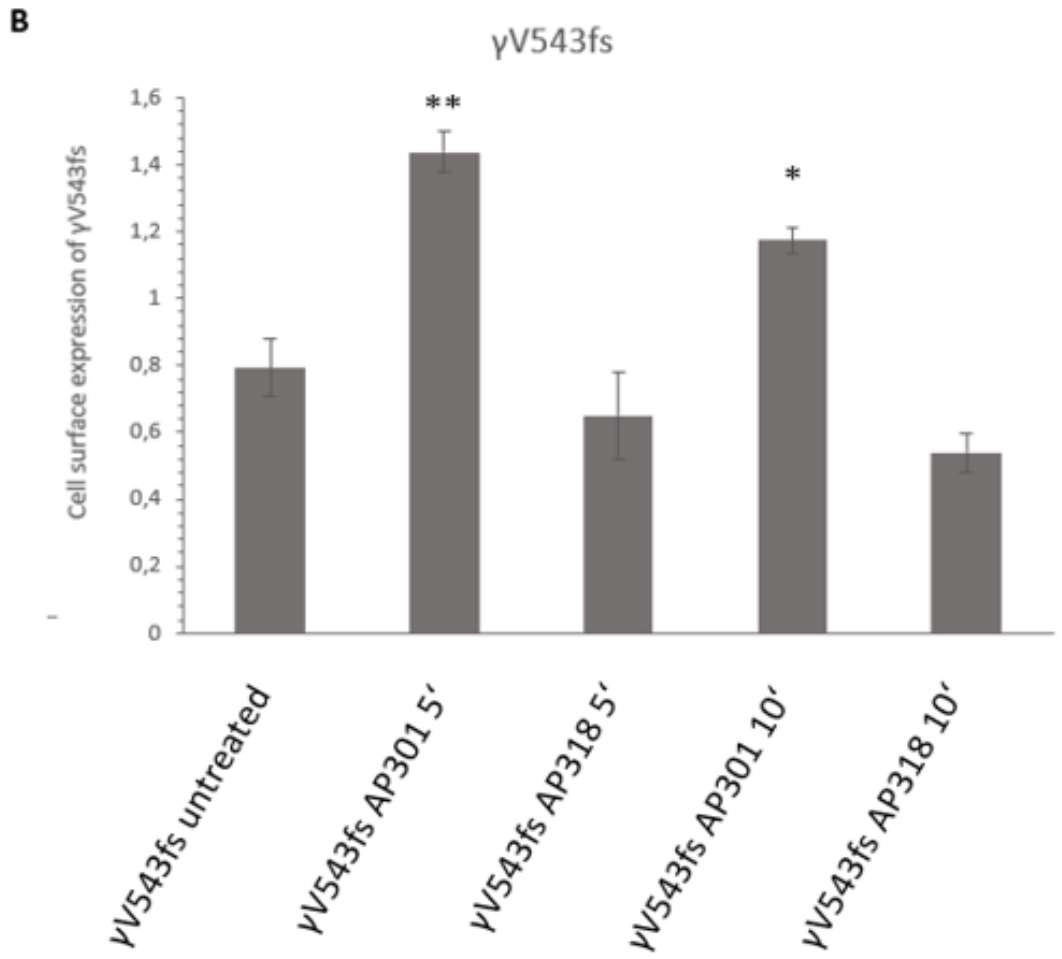

FIGURE 20. **Results for γV543fs(αβ)-hENaC after time-dependent treatment with AP301 and AP318.**

(A) Effect on membrane abundance of γV543fs(αβ)-hENaC after time-dependent treatment with AP301 and AP318 in transiently transfected HEK-293 cells.

γV543fs was co-expressed with WT (αβ)-ENaC in HEK-293 cells. Cells were treated with 200 nM AP301 and AP318 for 5 and 10 minutes each or untreated (control). After separation under reducing conditions by SDS-PAGE the biotinylated surface proteins were blotted semi-dry and visualized by immunoblotting with anti γ-ENaC antibodies. The truncated mutant is shorter than WT γ(αβ)-ENaC (75 kDa) and the line indicates the relevant band. β-tubulin shows a band at about 55 kDa and was used as loading control for relative quantification of the expression of γV543fs(αβ)-ENaC. Three blots were performed using independent biological replicants and one representative is shown.

(B) Densiometric analysis of γV543fs(αβ)-ENaC expression.

γV543fs(αβ)-ENaC was treated with 200 nM AP301 or AP318 for 5 or 10 minutes or not treated (control). The expression of γV543fs(αβ)-ENaC was normalized compared to β-tubulin and set in relation to mutant control. Results are shown as mean ± SEM. Significant differences are indicated, *$p < 0,05$ and **$p < 0,01$ (n=3).

5 Discussion

PHA1B, a rare, inherited, salt-wasting disease, is associated with mutations leading to a loss-of-function in the epithelial sodium channel (5, 103). In this study I observed frameshift mutations that are caused by a deletion or insertion of single bases in genes encoding ENaC subunits resulting in a truncated protein with a disturbed channel function. More precisely, I studied if the cell surface expression of truncated mutants lacking the carboxy terminal domain could be rescued by the TIP-mimicking peptides AP301 and AP318. Further studies have shown an activating effect on ENaC by the lectin-like domain (TIP) of TNF-α binding to the carboxy terminal domain of the α-subunit (95) as well as binding to N-glycosylation sites in the extracellular loop of the α-subunit (12). Hence the TIP-mimicking peptides AP301 (12, 96) and AP318 (12) require the glycosylated extracellular domain and the carboxy terminus for targeting ENaC.

5.1 Effect of TIP-mimicking peptides on cell surface abundance of WT α(βγ)-hENaC and α-frameshift mutants

A co-expression of at least three subunits is necessary for full channel activity (16, 46) but the α-subunit (and δ) is more important as it is the pore forming subunit (16, 18, 96). Therefore, I always transfected HEK-293 cells with α-mutant DNA and (βγ)-subunits DNA respectively with γ-mutant DNA and (αβ)-subunits DNA. Most of the mutations causing PHA1B are found in the α-subunit (13) and all the α-frameshift mutations I studied i.g. αY447fs, αS243fs, αP197fs and αR438fs are located in the extracellular loop (14, 123). The effect on the cell surface expression of the mutants varied a lot. A transient increase in the cell surface abundance with AP301 and AP318 was possible but after 10 minutes it started to decrease again concerning the mutants αY447fs with AP318, αS243fs with AP301 and AP318, αP197fs with AP301 and αR438fs with AP318. The cell surface abundance of WT α(βγ)-ENaC was transiently increased after the treatment with both substances as well. Sometimes the expression was even a bit higher after a 10-minute treatment than after 5 minutes concerning the mutants αY447fs with AP301, αP197fs with AP318 and αR438fs with AP301.

The transient increase in the cell surface abundance of the α-mutants after the treatment with AP318 and AP301 despite the lacking carboxy-terminus is possible due to the N-linked glycosylation sites still interacting with TIP-mimicking peptides. This thought is supported by

Willam et al. (13), who showed that after PNGase treatment (to remove N-glycosylation sites) of a mutant (αR448fs) lacking the carboxy terminus as well, neither an increase in the amiloride-sensitive sodium current nor a higher cell surface abundance was indicated.
Additionally, ENaC subunits need to preassemble in the ER to target to the membrane (46). The non-treated α-mutants show a higher expression or rather translocation than WT α(βγ) control, thus the mutations in the α-subunit probably have no effect on the channel assembly. Another possible explanation for the higher cell surface abundance could be the missing PY motif which is located in the carboxy-terminal domain (47). Without this conserved region the internalization of channels in the membrane is not possible, which in turn leads to a higher number of channels in the cell membrane (36, 48, 59).

5.2 Effect of TIP-mimicking peptides on the cell surface abundance of a γ-mutation in the TM2 region

Whereas the α-subunit is required for the channel activity the accessory β- and γ-subunit are important for surface activity and expression of the channel (121).
The γ-subunit is suggested to be more important for the cell surface expression, the channel assembly and ENaC trafficking of a functional ENaC than the β-subunit (15, 16, 42). Especially the N-terminus of γ-ENaC and the TM2 domain are important for channel formation (42). If any of these two regions are missing or mutated it is not possible to form a functional channel and it disturbs the function of the subunit (44). The γV543fs mutation is in the TM2 region and the following premature stop codon leads to the lack of the carboxy terminal domain (14). The mutant γV543fs showed a low cell surface abundance without any treatment and *Willam et al.* (14) described a low control current for this mutant as well, which indicates a severe loss-of-function. Even though a transient restoration of the cell surface abundance with AP301 was visible, there was no increase with AP318. In fact, an even lower cell surface abundance with AP318 occurred compared to the untreated mutant. Nevertheless, *Willam et al.* (14) showed an increase in the amiloride-sensitive sodium current with AP301 and an even higher increase with AP318. The surface expression of WT γ(αβ) did not show any significant increase with the TIP-mimicking peptides at all.
When expressed heterologously (as in HEK-293 cells) all three subunits are glycosylated (63), which indicates that all three show the same insertion into the membrane (23). But since the γV543fs mutation is found in the TM2 segment that is important for channel formation (42),

it is possible that the γ-mutant leads to a malfunction of the protein folding in the ER. Hence fewer ENaC proteins are found in the cell membrane. The current potentiating effect indicated for γV543fs with AP301 and AP318 (14) is therefore not due to a higher cell surface abundance. But still, the TIP-mimicking peptides can bind to N-glycosylation sites in the γ-subunit (12) and probably as well interact with the carboxy terminal domain in the α-subunit (122).

5.3 Potential binding sites of the TIP-mimicking peptides within ENaC and mechanisms of activity regulation

ENaC activity is regulated by two mechanisms: its inactive form is cleaved by different serine proteases to become the active protein and to be transferred to the plasma membrane from Golgi apparatus (76). The cleavage site is in the extracellular loop (75). The other mechanism of regulation is the ubiquitination, which is very important for the regulation of the cell surface expression of proteins (36, 59). The PY motif in the carboxy-terminal domain is required for Nedd4-2 to ubiquitinate the membrane epithelial sodium channels as a signal for internalization (48, 59). Since the PY motif is missing in all mutants, the ubiquitin ligase Nedd4 cannot bind to ENaC and without the ubiquitination an accumulation of the channels in the membrane is the consequence. This is a possible explanation for the fact that the non-treated α-mutants show an even higher abundance than WT α(βγ) control. The cell surface abundance of the non-treated γV543fs mutant was lower than WT control, which indicates a severe loss of function of this mutant perhaps due to a malfunction of protein folding in the ER since the mutation is found in the TM2 segment important for trafficking and channel assembly (42). Since all the frameshift mutants lack the carboxy terminal domain which is one binding site of the lectin-like domain (TIP) (95), it is crucial for the TIP domain to bind to N-glycosylation sites (12) to increase the translocation of the channels from the Golgi apparatus to the cell membrane and/or to activate ENaC.

The macroscopic current of ENaC is reliant on the number of channels in the membrane, intracellular trafficking of the channels and function of single channels like open probability (1, 52). Different experiments from the Department of Pharmacology and Toxicology indicate a benefiting effect for WT α(βγ) and the loss-of-function α- and γ-mutants after the treatment with AP301 and AP318 concerning electrophysiological experiments e.g. increase in amiloride-sensitive sodium current level up to or even higher than the untreated WT (12–14, 96). During

my work I found out that the effect on the cell surface expression of the mutants was not consistent. The number of mutant and WT epithelial sodium channels in the cell membrane was only transiently increased if it was increased at all. Thus the increase in cell surface abundance of the mutants and WT stands in no correlation with the increased amiloride-sensitive sodium current measured by *Willam et al*. (13, 14).

Hence I can deduce that the rescue of ENaC function is not because of a higher cell surface expression but rather because of a lower level of degradation or higher level of translocation from the Golgi apparatus to the cell membrane or change in single channel kinetics.

6 Conclusion

Although previous studies showed that the carboxy-terminus is one of the crucial sites for the interaction of TIP-mimicking peptides AP301 and AP318 with the epithelial sodium channel (95) there was still a transient increase in the cell membrane abundance of most of the investigated loss-of-function mutants lacking the carboxy-terminal domain and WT α(βγ) after the treatment with these substances. This increase may be due to less degradation as they lack the PY motif or due to a higher translocation rate of the channels concerning the α-mutants. The γV543 frameshift mutation found in the TM2 region which is important for channel assembly (42) showed a cell surface abundance lower than WT γ(αβ) even with AP318. This indicates a severe loss of function of the mutated protein. Even though I observed only a transient increase and not a consistent alternation in the cell surface abundance of WT-ENaC and the αY447fs, αS243fs, αP197fs, αR438fs and γV543fs mutants with AP301 and AP318, our department made promising results concerning the restoration of the activity/function of WT-ENaC and loss-of-function mutants by measuring a persistently increased amiloride-sensitive sodium current after treatment with these two peptides (12–14, 96).

7 Abstract

The epithelial sodium channel (ENaC), particularly in the kidney, is crucial for the sodium and water balance of the whole body. The reabsorption of sodium and water in the distal nephron is regulated by aldosterone through mineralocorticoid receptor-associated (MCR) changes in the transcription of the Na^+/K^+-ATPase and the α-subunit of the epithelial sodium channel. A loss-of-function of ENaC leads to different hereditary diseases due to its wide tissue distribution such as colon, kidney, alveoli, salivary glands and sweat glands. One of these channelopathies is pseudohypoaldosteronism type 1B (PHA1B), a very rare, salt-wasting disease characterized by symptoms like dehydration, hypotension, vomiting, metabolic acidosis and failure to thrive. Its manifestation persists into adulthood and patients affected by this disease need a lifelong medical treatment which so far has only been symptomatic. Although these symptoms are typical of hypoaldosteronism, the aldosterone and renin levels are elevated. The activity of the epithelial sodium channel is regulated by its presence in the cell membrane and its open probability.

The cyclic peptides AP301 (INN: solnatide) and AP318, which mimic the lectin-like domain (TIP) of TNF-α, have been shown to increase the amiloride-sensitive sodium current of loss-of-function phenotype ENaC. The aim of my thesis was to investigate if these synthetic TIP-peptides alter the cell surface expression of the frameshift mutants αY447fs, αR438fs, αS243fs, αP197fs, γV543fs despite their lacking carboxy terminus, which has previously been reported of being one site of interaction of the TIP-domain with ENaC. Although these mutations lead to a loss-of-function, the cell surface expression of these mutants in the α-subunit was always higher than wild type ENaC. But still, after the treatment with the TIP-peptides the cell surface abundance varied a lot, and mostly only a transient increase in the cell surface abundance was indicated. The effect on the γ-mutant, regarding the cell surface expression as well as the amiloride-sensitive sodium current, indicated a complete loss-of-function of this mutant. Nevertheless patch-clamp experiments on these loss-of-function mutations in the α-subunit were promising and showed a restoration of the channel function. Therefore, one can deduce that the restoration of ENaC function is above all due to a higher open probability and not because of a higher cell surface expression. The activity of loss-of-function phenotype ENaC can be restored, hence AP301 and AP318 are promising substances for the treatment of PHA1B.

8 Zusammenfassung

Der epitheliale Natriumkanal (ENaC), vor allem in der Niere, ist entscheidend für die Balance des Natrium- und Wasserhaushalts im ganzen Körper. Die Rückresorption von Natrium und Wasser im distalen Nephron wird von Aldosteron durch mineralkortikoidrezeptor-abhängige Veränderungen in der Transkriptionsrate der Na^+/K^+-ATPase und der α-Untereinheit des ENaCs reguliert. Ein Funktionsverlust des ENaC führt zu unterschiedlichen Erbkrankheiten. Eine dieser ist Pseudohypoaldosteronismus Typ 1B (PHA1B), eine sehr seltene, einen Salzverlust hervorrufende Krankheit, die durch Symptome wie Dehydration, Hypotonie, Erbrechen, metabolische Azidose und Gedeihstörungen gekennzeichnet ist. Ihre Manifestation bleibt bis ins Erwachsenenalter bestehen und Patienten, die von dieser Krankheit betroffen sind, benötigen lebenslange medizinische Behandlung, welche bis jetzt nur symptomatisch erfolgt ist. Obwohl die Symptome typisch für Hypoaldosteronismus sind, sind die Aldosteron- und Reninwerte erhöht. Die Aktivität vom ENaC wird durch die Anzahl der Kanäle in der Zellmembran und deren Öffnungswahrscheinlichkeit reguliert. Die zyklischen Peptide AP301 (Solnatid) und AP318, welche die lektin-ähnliche Domäne (TIP) von TNF-α nachahmen, zeigten eine Erhöhung des Amilorid-sensitiven Natriumstroms von Loss-of-Function ENaC-Mutationen. Meine Arbeit zielte darauf ab, die Veränderungen der Oberflächenexpression der Frameshift-Mutanten αY447fs, αR438fs, αS243fs, αP197fs, γV543fs zu beobachten, welche keinen Carboxy-Terminus aufweisen. In früheren Studien wurde dieser als eine der Bindungsstellen der TIP-Peptide mit ENaC beschrieben. Obwohl diese Mutationen zu einem Funktionsverlust führen, war die Oberflächenexpression der α-Mutanten höher als die des Wildtyps. Dennoch variierte die Menge der Kanäle in der Zellmembran nach der Behandlung mit den TIP-Peptiden sehr. Meist war auch nur eine transiente Erhöhung der Oberflächenexpression zu sehen. Der Effekt auf die Oberflächenexpression als auch den Amilorid-sensitiven Natriumstrom der γ-Mutante wies auf einen kompletten Funktionsverlust dieser hin. Nichtsdestotrotz waren Patch-Clamp-Versuche an den α-Mutanten vielversprechend und zeigten eine Wiederherstellung der Kanalfunktion. Folglich kann daraus abgeleitet werden, dass die Wiederherstellung der ENaC-Funktion vor allem auf einer erhöhten Öffnungswahrscheinlichkeit und nicht auf einer erhöhten Oberflächenexpression der einzelnen Kanäle beruht. Da die Aktivität von Loss-of-Function ENaC-Mutationen wiederhergestellt werden konnte, können AP301 und AP318 als vielversprechende Substanzen zur Behandlung von PHA1B gesehen werden.

9 Appendix

9.1 Amino acid sequences of ENaC subunits and marked glycosylation sites

amino acid sequences from uniport.org with possible N-glycosylation sites (Asp-X-Ser/Thr)

SCNN1A_HUMAN amino acids: 1–669
extracellular: 107–562
(https://www.uniprot.org/uniprot/P37088)

```
        10         20         30         40         50
MEGNKLEEQD SSPPQSTPGL MKGNKREEQG LGPEPAAPQQ PTAEEEALIE
        60         70         80         90        100
FHRSYRELFE FFCNNTTIHG AIRLVCSQHN RMKTAFWAVL WLCTFGMMYW
       110        120        130        140        150
QFGLLFGEYF SYPVSLNINL NSDKLVFPAV TICTLNPYRY PEIKEELEEL
       160        170        180        190        200
DRITEQTLFD LYKYSSFTTL VAGSRSRRDL RGTLPHPLQR LRVPPPPHGA
       210        220        230        240        250
RRARSVASSL RDNNPQVDWK DWKIGFQLCN QNKSDCFYQT YSSGVDAVRE
       260        270        280        290        300
WYRFHYINIL SRLPETLPSL EEDTLGNFIF ACRFNQVSCN QANYSHFHHP
       310        320        330        340        350
MYGNCYTFND KNNSNLWMSS MPGINNGLSL MLRAEQNDFI PLLSTVTGAR
       360        370        380        390        400
VMVHGQDEPA FMDDGGFNLR PGVETSISMR KETLDRLGGD YGDCTKNGSD
       410        420        430        440        450
VPVENLYPSK YTQQVCIHSC FQESMIKECG CAYIFYPRPQ NVEYCDYRKH
       460        470        480        490        500
SSWGYCYYKL QVDFSSDHLG CFTKCRKPCS VTSYQLSAGY SRWPSVTSQE
       510        520        530        540        550
WVFQMLSRQN NYTVNNKRNG VAKVNIFFKE LNYKTNSESP SVTMVTLLSN
       560        570        580        590        600
LGSQWSLWFG SSVLSVVEMA ELVFDLLVIM FLMLLRRFRS RYWSPGRGGR
       610        620        630        640        650
GAQEVASTLA SSPPSHFCPH PMSLSLSQPG PAPSPALTAP PPAYATLGPR
       660
PSPGGSAGAS SSTCPLGGP
```

SCNN1B_HUMAN amino acids: 1–640
extracellular: 72–532
(https://www.uniprot.org/uniprot/P51168)

```
        10         20         30         40         50
MHVKKYLLKG LHRLQKGPGY TYKELLVWYC DNTNTHGPKR IICEGPKKKA
        60         70         80         90        100
MWFLLTLLFA ALVCWQWGIF IRTYLSWEVS VSLSVGFKTM DFPAVTICNA
       110        120        130        140        150
SPFKYSKIKH LLKDLDELME AVLERILAPE LSHANATRNL NFSIWNHTPL
       160        170        180        190        200
VLIDERNPHH PMVLDLFGDN HNGLTSSSAS EKICNAHGCK MAMRLCSLNR
       210        220        230        240        250
TQCTFRNFTS ATQALTEWYI LQATNIFAQV PQQELVEMSY PGEQMILACL
       260        270        280        290        300
FGAEPCNYRN FTSIFYPHYG NCYIFNWGMT EKALPSANPG TEFGLKLILD
       310        320        330        340        350
IGQEDYVPFL ASTAGVRLML HEQRSYPFIR DEGIYAMSGT ETSIGVLVDK
       360        370        380        390        400
LQRMGEPYSP CTVNGSEVPV QNFYSDYNTT YSIQACLRSC FQDHMIRNCN
       410        420        430        440        450
CGHYLYPLPR GEKYCNNRDF PDWAHCYSDL QMSVAQRETC IGMCKESCND
       460        470        480        490        500
TQYKMTISMA DWPSEASEDW IFHVLSQERD QSTNITLSRK GIVKLNIYFQ
       510        520        530        540        550
EFNYRTIEES AANNIVWLLS NLGGQFGFWM GGSVLCLIEF GEIIIDFVWI
       560        570        580        590        600
TIIKLVALAK SLRQRRAQAS YAGPPPTVAE LVEAHTNFGF QPDTAPRSPN
       610        620        630        640
TGPYPSEQAL PIPGTPPPNY DSLRLQPLDV IESDSEGDAI
```

SCNN1G_HUMAN amino acids: 1–649
extracellular: 77–541
(https://www.uniprot.org/uniprot/P51170)

```
        10         20         30         40         50
MAPGEKIKAK IKKNLPVTGP QAPTIKELMR WYCLNTNTHG CRRIVVSRGR
        60         70         80         90        100
LRRLLWIGFT LTAVALILWQ CALLVFSFYT VSVSIKVHFR KLDFPAVTIC
       110        120        130        140        150
NINPYKYSTV RHLLADLEQE TREALKSLYG FPESRKRREA ESWNSVSEGK
       160        170        180        190        200
QPRFSHRIPL LIFDQDEKGK ARDFFTGRKR KVGGSIIHKA SNVMHIESKQ
       210        220        230        240        250
VVGFQLCSND TSDCATYTFS SGINAIQEWY KLHYMNIMAQ VPLEKKINMS
       260        270        280        290        300
YSAEELLVTC FFDGVSCDAR NFTLFHHPMH GNCYTFNNRE NETILSTSMG
```

```
        310         320         330         340         350
GSEYGLQVIL YINEEEYNPF LVSSTGAKVI IHRQDEYPFV EDVGTEIETA
        360         370         380         390         400
MVTSIGMHLT ESFKLSEPYS QCTEDGSDVP IRNIYNAAYS LQICLHSCFQ
        410         420         430         440         450
TKMVEKCGCA QYSQPLPPAA NYCNYQQHPN WMYCYYQLHR AFVQEELGCQ
        460         470         480         490         500
SVCKEACSFK EWTLTTSLAQ WPSVVSEKWL LPVLTWDQGR QVNKKLNKTD
        510         520         530         540         550
LAKLLIFYKD LNQRSIMESP ANSIEMLLSN FGGQLGLWMS CSVVCVIEII
        560         570         580         590         600
EVFFIDFFSI IARRQWQKAK EWWAWKQAPP CPEAPRSPQG QDNPALDIDD
        610         620         630         640
DLPTFNSALH LPPALGTQVP GTPPPKYNTL RLERAFSNQL TDTQMLDEL
```

SCNN1D_HUMAN 1–638 (http://www.uniprot.org/uniprot/P51172)
extracellular: 108–530

```
   10          20          30          40          50
MAEHRSMDGR MEAATRGGSH LQAAAQTPPR PGPPSAPPPP PKEGHQEGLV
          60          70          80          90         100
ELPASFRELL TFFCTNATIH GAIRLVCSRG NRLKTTSWGL LSLGALVALC
         110         120         130         140         150
WQLGLLFERH WHRPVLMAVS VHSERKLLPL VTLCDGNPRR PSPVLRHLEL
         160         170         180         190         200
LDEFARENID SLYNVNLSKG RAALSATVPR HEPPFHLDRE IRLQRLSHSG
         210         220         230         240         250
SRVRVGFRLC NSTGGDCFYR GYTSGVAAVQ DWYHFHYVDI LALLPAAWED
         260         270         280         290         300
SHGSQDGHFV LSCSYDGLDC QARQFRTFHH PTYGSCYTVD GVWTAQRPGI
         310         320         330         340         350
THGVGLVLRV EQQPHLPLLS TLAGIRVMVH GRNHTPFLGH HSFSVRPGTE
         360         370         380         390         400
ATISIREDEV HRLGSPYGHC TAGGEGVEVE LLHNTSYTRQ ACLVSCFQQL
         410         420         430         440         450
MVETCSCGYY LHPLPAGAEY CSSARHPAWG HCFYRLYQDL ETHRLPCTSR
         460         470         480         490         500
CPRPCRESAF KLSTGTSRWP SAKSAGWTLA TLGEQGLPHQ SHRQRSSLAK
         510         520         530         540         550
INIVYQELNY RSVEEAPVYS VPQLLSAMGS LCSLWFGASV LSLLELLELL
         560         570         580         590         600
LDASALTLVL GGRRLRRAWF SWPRASPASG ASSIKPEASQ MPPPAGGTSD
         610         620         630
DPEPSGPHLP RVMLPGVLAG VSAEESWAGP QPLETLDT
```

9.2 List of abbreviations

A549	adenocarcinomic human alveolar basal epithelial cell
AP301	solnatide
APS	ammonium persulfate
ASIC1	acid-sensing ion channel 1
ASL	airway liquid surface
Asn-X-Ser/Thr	asparagine-X-Serine/Threonine, (consensus sequence for N-glycosylation)
BSA	bovine serum albumin
C2-domain	Ca^{2+}-binding motif
cAMP	cyclic adenosine monophosphate
CD	collecting duct
CF	cystic fibrosis
CFTR	cystic fibrosis transmembrane conductance regulator
CNT	connecting tubule
CRD	cysteine-rich domain
DEG	degenerins
del	deletion
DMEM	Dulbecco's Modified Eagle Medium
ECD	extracellular domain
ECL	enhanced chemiluminescence
ENaC	epithelial sodium channel
ER	endoplasmic reticulum
ERK1/2	extracellular signal-regulated kinases
FaNaC	FMRFamide-gated Sodium Channel
FBS	fetal bovine serum
GILZ1	glucocorticoid-induced leucine zipper protein 1
Gly/Ser-X-Ser motif	glycine/serine-X-serine
H^+	proton
HECT-domain	homologous to the E6-AP carboxyl terminus (domain in ubiquitin-protein ligases)
HEK-293 cells	human embryonic kidney cells
hENaC	human epithelial sodium channel
HG-motif	histidine/glycine-motif
HRP	horse-radish peroxidase
hTNF-α	human tumor necrosis factor alpha
ins	insertion
i.v.	intravenous
K^+	potassium
kDA	kilo Dalton
Li^+	lithium
mAB	monoclonal antibody
MARCKS	myristoylated alanine-rich C-kinase substrate
MCR	mineralocorticoid receptor
MEK1/2	mitogen-activated kinase/ERK kinase 1/2
Na^+	sodium
Na^+/K^+-ATPase	sodium-potassium adenosine triphosphatase

Nedd4-2	neural precursor cell expressed, developmentally down-regulated protein 4, E3 ubiquitin protein ligase
NR3C2	nuclear receptor subfamily 3, group C, member 2
Po	open probability
P1, P2	proline-rich-segments
PBS	phosphate buffered saline
PHA1	pseudohypoaldosteronism type 1
PIP2	phosphatidylinositol-4,5-bisphosphate
PKA	protein kinase A
postM1	short stretch of amino acid residues following the putative transmembrane domain TM1
preM2	short stretch of amino acid residues preceding the putative second transmembrane domain TM2
PY-motif	sequence that binds ubiquitin-protein ligase
Raf-1	v-raf-1 murine leukaemia viral oncogene homolog 1
SCN1	sodium voltage-gated channel 1
SCNN1	sodium channel, non-neuronal 1
SDS-PAGE	Sodium dodecylsulfate-polyacrylamide gel electrophoresis
SEM	standard error of the mean
SGK1	serum and glucocorticoid-regulated kinase 1
TBS	tris buffered saline
TEMED	tetramethyl-ethylene-diamine
TIP	lectin-like domain of TNF-α
TM1/2	transmembrane domain 1/2
TNF-α	tumor necrosis factor alpha
TRIS	tris(hydroxymethyl)aminomethane
WT	wild type
WW domain	rsp5-domain or WWP repeating motif (protein domain)

9.3 Used drugs/chemical reagents and their providers

Substance	Provider
Dulbecco's modified Eagle medium/F12 nutrient mixture Ham plus L-glutamine	Gibco™ by Life Technologies, LifeTech Austria
Fetal bovine serum	Gibco™ by Life Technologies, LifeTech Austria
Penicillin-streptomycin 1:1	Sigma-Aldrich GmbH, Vienna, Austria
PBS without calcium and magnesium pH 7,4	Thermo Fisher, Rockford, USA
Trypsin/EDTA 0,05%	Gibco™ by Life Technologies, LifeTech Austria
X-tremeGENE™ HP DNA transfection reagent	Roche Diagnostics, Mannheim, Germany
Serum-free DMEM	Gibco™ by Life Technologies, LifeTech Austria
α-wt, β-wt, γ-wt, αY447fs, αS243fs, αP197fs, αR438fs, γV543fs	Snyder's DNA, University of Iowa, Carver College of Medicine, Iowa City, USA
Biotinylation Kit	Thermo Scientific, Rockford, USA
Color-coded prestained protein marker, High Range (43–315 kDa)	Cell Signaling Technology®
Anti-α-EnaC from goat	Santa Cruz Biotechnology, Texas USA
Anti-goat IgG, HRP-linked from donkey	Santa Cruz Biotechnology, Texas USA
Anti-α-EnaC from rabbit	Sigma
Anti-rabbit IgG, HRP-linked from goat	Santa Cruz Biotechnology, Texas USA
Anti-γ-EnaC from goat	Sigma
Anti-β-Tubulin from mouse	Sigma
Anti-mouse IgG, HRP-linked from goat	Sigma
AP301, AP318	APEPTICO
Enhanced chemiluminescence (ECL) substrate	Amersham ECL Plus Western Blotting Detection Reagent, GE Healthcare, Vienna, Austria

9.4 LIST OF TABLES

9.5 LIST OF FIGURES

9.6 REFERENCES

1. Garty H, Palmer LG. Epithelial sodium channels: Function, structure, and regulation. *Physiol Rev* (1997) **77**(2):359–96. doi:10.1152/physrev.1997.77.2.359

2. McNicholas CM, Canessa CM. Diversity of Channels Generated by Different Combinations of Epithelial Sodium Channel Subunits. *J Gen Physiol* (1997) **109**(6):681–92.

3. Bhalla V, Hallows KR. Mechanisms of ENaC Regulation and Clinical Implications. *JASN* (2008) **19**(10):1845–54.

4. Firsov D, Schild L, Gautschi I, Mérillat AM, Schneeberger E, Rossier BC. Cell surface expression of the epithelial Na channel and a mutant causing Liddle syndrome: A quantitative approach. *Proc Natl Acad Sci U S A* (1996) **93**(26):15370–5.

5. Amin N, Alvi NS, Barth JH, Field HP, Finlay E, Tyerman K, et al. Pseudohypoaldosteronism type 1: Clinical features and management in infancy. *Endocrinol Diabetes Metab Case Rep* (2013) **2013**:130010. doi:10.1530/EDM-13-0010

6. König J, Schreiber R, Voelcker T, Mall M, Kunzelmann K. The cystic fibrosis transmembrane conductance regulator (CFTR) inhibits ENaC through an increase in the intracellular Cl- concentration. *EMBO Rep* (2001) **2**(11):1047–51. doi:10.1093/embo-reports/kve232

7. Matthay MA, Folkesson HG, Clerici C. Lung epithelial fluid transport and the resolution of pulmonary edema. *Physiol Rev* (2002) **82**(3):569–600. doi:10.1152/physrev.00003.2002

8. Dillon MJ, Leonard JV, Buckler JM, Ogilvie D, Lillystone D, Honour JW, Shackleton CH. Pseudohypoaldosteronism. *Arch Dis Child* (1980) **55**(6):427–34.

9. Hribar M, Bloc A, van der Goot FG, Fransen L, Baetselier P de, Grau GE, et al. The lectin-like domain of tumor necrosis factor-α increases membrane conductance in microvascular endothelial cells and peritoneal macrophages. *Eur. J. Immunol.* (1999) **29**(10):3105–11. doi:10.1002/(SICI)1521-4141(199910)29:10<3105:AID-IMMU3105>3.0.CO;2-A

10. Fukuda N, Jayr C, Lazrak A, Wang Y, Lucas R, Matalon S, et al. Mechanisms of TNF-alpha stimulation of amiloride-sensitive sodium transport across alveolar epithelium. *Am J Physiol Lung Cell Mol Physiol* (2001) **280**(6):L1258-65. doi:10.1152/ajplung.2001.280.6.L1258

11. Hazemi P, Tzotzos SJ, Fischer B, Andavan GS, Fischer H, Pietschmann H, et al. Essential structural features of TNF-α lectin-like domain derived peptides for activation of amiloride-sensitive sodium current in A549 cells. *J Med Chem* (2010) **53**(22):8021–9. doi:10.1021/jm100767p

12. Shabbir W, Tzotzos Se. Glycosylation-dependent activation of epithelial sodium channel by solnatide. *Elsevier Biochemical Pharmacology* (2015) **98**(4):740–53.

13. Willam A, Aufy M, Tzotzos S, El-Malazi D, Poser F, Wagner A, et al. TNF Lectin-Like Domain Restores Epithelial Sodium Channel Function in Frameshift Mutants Associated with Pseudohypoaldosteronism Type 1B. *Front Immunol* (2017) **8**:601. doi:10.3389/fimmu.2017.00601

14. Willam A, Aufy M, Tzotzos S, Evanzin H, Chytracek S, Geppert S, et al. Restoration of Epithelial Sodium Channel Function by Synthetic Peptides in Pseudohypoaldosteronism Type 1B Mutants. *Front Pharmacol* (2017) **8**. doi:10.3389/fphar.2017.00085

15. Giraldez T, Rojas P, Jou J, Flores C, La Alvarez de Rosa D. The epithelial sodium channel δ-subunit: New notes for an old song. *Am J Physiol Renal Physiol* (2012) **303**(3):F328-338. doi:10.1152/ajprenal.00116.2012

16. Canessa CM, Schild L, Buell G, Thorens B, Gautschi I, Horisberger JD, et al. Amiloride-sensitive epithelial Na+ channel is made of three homologous subunits. *Nature* (1994) **367**(6462):463–7. doi:10.1038/367463a0

17. Canessa CM, Horisberger JD, Rossier BC. Epithelial sodium channel related to proteins involved in neurodegeneration. *Nature* (1993) **361**(6411):467–70. doi:10.1038/361467a0

18. Waldmann R, Champigny G, Bassilana F, Voilley N, Lazdunski M. Molecular cloning and functional expression of a novel amiloride-sensitive Na+ channel. *J Biol Chem* (1995) **270**(46):27411–4.

19. Schild L, Firsov D, Gautschi I, Merillat AM, Rossier BC. The heterotetrameric architecture of the epithelial sodium channel (ENaC). *EMBO J* (1998) **17**(2):344–52. doi:10.1093/emboj/17.2.344

20. McDonald FJ, Price MP, Snyder PM, Welsh MJ. Cloning and expression of the beta- and gamma-subunits of the human epithelial sodium channel. *American Journal of Physiology - Cell Physiology* (1995) **268**(5):C1157-C1163.

21. Kosari F, Sheng S, Li J, Mak D-OD, Foskett JK, Kleyman TR. Subunit Stoichiometry of the Epithelial Sodium Channel. *J. Biol. Chem.* (1998) **273**(22):13469–74. doi:10.1074/jbc.273.22.13469

22. Snyder PM, Cheng C, Prince LS, Rogers JC, Welsh MJ. Electrophysiological and Biochemical Evidence That DEG/ENaC Cation Channels Are Composed of Nine Subunits. *J. Biol. Chem.* (1998) **273**(2):681–4. doi:10.1074/jbc.273.2.681

23. Canessa CM, Merillat AM, Rossier BC. Membrane topology of the epithelial sodium channel in intact cells. *Am J Physiol* (1994) **267**(6 Pt 1):C1682-90.

24. Kashlan OB, Kleyman TR. ENaC structure and function in the wake of a resolved structure of a family member. *Am J Physiol Renal Physiol* (2011) **301**(4):F684-96. doi:10.1152/ajprenal.00259.2011

25. Ben-Shahar Y. Sensory functions for degenerin/epithelial sodium channels (DEG/ENaC). *Adv Genet* (2011) **76**:1–26. doi:10.1016/B978-0-12-386481-9.00001-8

26. Hanukoglu I, Hanukoglu A. Epithelial sodium channel (ENaC) family: Phylogeny, structure-function, tissue distribution, and associated inherited diseases. *Gene* (2016) **579**(2):95–132.

27. Jasti J, Furukawa H, Gonzales EB, Gouaux E. Structure of acid-sensing ion channel 1 at 1.9 A resolution and low pH. *Nature* (2007) **449**(7160):316–23. doi:10.1038/nature06163

28. Huang M, Chalfie M. Gene interactions affecting mechanosensory transduction in Caenorhabditis elegans. *Nature* (1994) **367**(6462):467–70. doi:10.1038/367467a0

29. Take-uchi M, Kawakami M, Ishihara T, Amano T, Kondo K, Katsura I. An ion channel of the degenerin/epithelial sodium channel superfamily controls the defecation rhythm in Caenorhabditis elegans. *Proc Natl Acad Sci U S A* (1998) **95**(20):11775–80.

30. Lingueglia E, Champigny G, Lazdunski M, Barbry P. Cloning of the amiloride-sensitive FMRFamide peptide-gated sodium channel. *Nature* (1995) **378**(6558):730–3. doi:10.1038/378730a0

31. Chen J, Kleyman TR, Sheng S. Deletion of α-subunit exon 11 of the epithelial Na+ channel reveals a regulatory module. *Am J Physiol Renal Physiol* (2014) **306**(5):F561-7. doi:10.1152/ajprenal.00587.2013

32. Kellenberger S, Schild L. International Union of Basic and Clinical Pharmacology. XCI. structure, function, and pharmacology of acid-sensing ion channels and the epithelial Na+ channel. *Pharmacol Rev* (2015) **67**(1):1–35. doi:10.1124/pr.114.009225

33. Gründer S, Pusch M. Biophysical properties of acid-sensing ion channels (ASICs). *Neuropharmacology* (2015) **94**:9–18. doi:10.1016/j.neuropharm.2014.12.016

34. Waldmann R, Lazdunski M. H(+)-gated cation channels: Neuronal acid sensors in the NaC/DEG family of ion channels. *Curr Opin Neurobiol* (1998) **8**(3):418–24.

35. Reeh PW, Steen KH. Tissue acidosis in nociception and pain. *Prog Brain Res* (1996) **113**:143–51.

36. Kellenberger S, Schild L. Epithelial sodium channel/degenerin family of ion channels: A variety of functions for a shared structure. *Physiol Rev* (2002) **82**(3):735–67. doi:10.1152/physrev.00007.2002

37. Palmer LG. Ion selectivity of the apical membrane Na channel in the toad urinary bladder. *J Membr Biol* (1982) **67**(2):91–8.

38. Kellenberger S, Schild Le. Permeability Properties of Enac Selectivity Filter Mutants. *J Gen Physiol.* (2001) **118**(6):679–92.

39. Snyder PM, Olson DR, Bucher DB. A Pore Segment in DEG/ENaC Na + Channels. *J. Biol. Chem.* (1999) **274**(40):28484–90. doi:10.1074/jbc.274.40.28484

40. Alvarez de la Rosa, D., Canessa CM, Fyfe GK, Zhang P. Structure and regulation of amiloride-sensitive sodium channels. *Annu Rev Physiol* (2000) **62**:573–94. doi:10.1146/annurev.physiol.62.1.573

41. Schild L, Schneeberger E, Gautschi I, Firsov D. Identification of amino acid residues in the alpha, beta, and gamma subunits of the epithelial sodium channel (ENaC) involved in amiloride block and ion permeation. *J Gen Physiol* (1997) **109**(1):15–26.

42. Konstas A-A, Korbmacher C. The gamma-subunit of ENaC is more important for channel surface expression than the beta-subunit. *Am J Physiol Cell Physiol* (2003) **284**(2):C447-56. doi:10.1152/ajpcell.00385.2002

43. Heijne G vGeering. Oligomerization and Maturation of Eukaryotic Membrane Proteins (1996):173–88.

44. Adams CM, Snyder PM, Welsh MJ. Interactions between Subunits of the Human Epithelial Sodium Channel. *J. Biol. Chem.* (1997) **272**(43):27295–300. doi:10.1074/jbc.272.43.27295

45. Firsov D, Robert-Nicoud M, Gruender S, Schild L, Rossier BC. Mutational analysis of cysteine-rich domains of the epithelium sodium channel (ENaC). Identification of cysteines essential for channel expression at the cell surface. *J. Biol. Chem.* (1999) **274**(5):2743–9.

46. Snyder PM, McDonald FJ, Stokes JB, Welsh MJ. Membrane topology of the amiloride-sensitive epithelial sodium channel. *J. Biol. Chem.* (1994) **269**(39):24379–83.

47. Schild L, Lu Y, Gautschi I, Schneeberger E, Lifton RP, Rossier BC. Identification of a PY motif in the epithelial Na channel subunits as a target sequence for mutations causing channel activation found in Liddle syndrome. *EMBO J* (1996) **15**(10):2381–7.

48. Goulet CC, Volk KA, Adams CM, Prince LS, Stokes JB, Snyder PM. Inhibition of the Epithelial Na+ Channel by Interaction of Nedd4 with a PY Motif Deleted in Liddle's Syndrome. *J. Biol. Chem.* (1998) **273**(45):30012–7. doi:10.1074/jbc.273.45.30012

49. Duc C, Farman N, Canessa CM, Bonvalet JP, Rossier BC. Cell-specific expression of epithelial sodium channel alpha, beta, and gamma subunits in aldosterone-responsive

epithelia from the rat: Localization by in situ hybridization and immunocytochemistry. *The Journal of Cell Biology* (1994) **127**(6):1907. doi:10.1083/jcb.127.6.1907

50. Li X-J, Blackshaw Se. Expression and localization of amiloride-sensitive sodium channel indicate a role for non-taste cells in taste perception. *Proc. Nati. Acad. Sci. USA Neurobiology* (1994) **91**:1814–8.

51. Marunaka Y. Characteristics and Pharmacological Regulation of Epithelial Na+ Channel (ENaC) and Epithelial Na+ Transport. *Journal of Pharmacological Sciences* (2014) **126**. doi:10.1254/jphs.14R01SR

52. Gormley K, Dong Y, Sagnella GA. Regulation of the epithelial sodium channel by accessory proteins. *Biochem J* (2003) **371**(Pt 1):1–14. doi:10.1042/BJ20021375

53. Shigaev A, Asher C, Latter H, Garty H, Reuveny E. Regulation of sgk by aldosterone and its effects on the epithelial Na(+) channel. *Am J Physiol Renal Physiol* (2000) **278**(4):F613-9. doi:10.1152/ajprenal.2000.278.4.F613

54. Ecelbarger CA, Kim GH, Wade JB, Knepper MA. Regulation of the abundance of renal sodium transporters and channels by vasopressin. *Exp Neurol* (2001) **171**(2):227–34. doi:10.1006/exnr.2001.7775

55. Gilmore ES, Stutts MJ, Milgram SL. SRC family kinases mediate epithelial Na+ channel inhibition by endothelin. *J. Biol. Chem.* (2001) **276**(45):42610–7. doi:10.1074/jbc.M106919200

56. Lang F, Strutz-Seebohm N, Seebohm G, Lang UE. Significance of SGK1 in the regulation of neuronal function. *J Physiol (Lond)* (2010) **588**(Pt 18):3349–54. doi:10.1113/jphysiol.2010.190926

57. Debonneville C, Flores SY, Kamynina E, Plant PJ, Tauxe C, Thomas MA, et al. Phosphorylation of Nedd4-2 by Sgk1 regulates epithelial Na(+) channel cell surface expression. *EMBO J* (2001) **20**(24):7052–9. doi:10.1093/emboj/20.24.7052

58. Soundararajan R, Zhang TT, Wang J, Vandewalle A, Pearce D. A novel role for glucocorticoid-induced leucine zipper protein in epithelial sodium channel-mediated sodium transport. *J. Biol. Chem.* (2005) **280**(48):39970–81. doi:10.1074/jbc.M508658200

59. Staub O, Abriel H, Plant P, Ishikawa T, Kanelis V, Saleki R, et al. Regulation of the epithelial Na+ channel by Nedd4 and ubiquitination. *Kidney Int* (2000) **57**(3):809–15. doi:10.1046/j.1523-1755.2000.00919.x

60. Staub O, Dho S, Henry P, Correa J, Ishikawa T, McGlade J, et al. WW domains of Nedd4 bind to the proline-rich PY motifs in the epithelial Na+ channel deleted in Liddle's syndrome. *EMBO J* (1996) **15**(10):2371–80.

61. Hansson JH, Nelson-Williams C, Suzuki H, Schild L, Shimkets R, Lu Y, et al. Hypertension caused by a truncated epithelial sodium channel gamma subunit: Genetic heterogeneity of Liddle syndrome. *Nat Genet* (1995) **11**(1):76–82. doi:10.1038/ng0995-76

62. Yu H. Structural basis for the binding of proline-rich peptides to SH3 domains. *Cell* (1994) **76**(5):933–45. doi:10.1016/0092-8674(94)90367-0

63. Staub O, Gautschi I, Ishikawa T, Breitschopf K, Ciechanover A, Schild L, et al. Regulation of stability and function of the epithelial Na+ channel (ENaC) by ubiquitination. *EMBO J* (1997) **16**(21):6325–36. doi:10.1093/emboj/16.21.6325

64. Ciechanover A. The ubiquitin-proteasome proteolytic pathway. *Cell* (1994) **79**(1):13–21. doi:10.1016/0092-8674(94)90396-4

65. Asher C, Wald H, Rossier BC, Garty H. Aldosterone-induced increase in the abundance of Na+ channel subunits. *Am J Physiol* (1996) **271**(2 Pt 1):C605-11. doi:10.1152/ajpcell.1996.271.2.C605

66. Plant PJ, Yeger H, Staub O, Howard P, Rotin D. The C2 Domain of the Ubiquitin Protein Ligase Nedd4 Mediates Ca 2+ -dependent Plasma Membrane Localization. *J. Biol. Chem.* (1997) **272**(51):32329–36. doi:10.1074/jbc.272.51.32329

67. Butterworth MB, Edinger RS, Johnson JP, Frizzell RA. Acute ENaC stimulation by cAMP in a kidney cell line is mediated by exocytic insertion from a recycling channel pool. *J Gen Physiol* (2005) **125**(1):81–101. doi:10.1085/jgp.200409124

68. Taruno A, Marunaka Y. Analysis of blocker-labeled channels reveals the dependence of recycling rates of ENaC on the total amount of recycled channels. *Cell Physiol Biochem* (2010) **26**(6):925–34. doi:10.1159/000324001

69. Falin R, Veizis IE, Cotton CU. A role for ERK1/2 in EGF- and ATP-dependent regulation of amiloride-sensitive sodium absorption. *Am J Physiol Cell Physiol* (2005) **288**(5):C1003-11. doi:10.1152/ajpcell.00213.2004

70. Soundararajan R, Melters D, Shih I-C, Wang J, Pearce D. Epithelial sodium channel regulated by differential composition of a signaling complex. *Proc Natl Acad Sci U S A* (2009) **106**(19):7804–9. doi:10.1073/pnas.0809892106

71. Morris RG, Schafer JA. cAMP Increases Density of ENaC Subunits in the Apical Membrane of MDCK Cells in Direct Proportion to Amiloride-sensitive Na + Transport. *J Gen Physiol* (2002) **120**(1):71–85. doi:10.1085/jgp.20018547

72. Nielsen S, Frøkiaer J, Marples D, Kwon T-H, Agre P, Knepper MA. Aquaporins in the kidney: From molecules to medicine. *Physiol Rev* (2002) **82**(1):205–44. doi:10.1152/physrev.00024.2001

73. Escoubet B, Coureau C, Bonvalet JP, Farman N. Noncoordinate regulation of epithelial Na channel and Na pump subunit mRNAs in kidney and colon by aldosterone. *Am J Physiol* (1997) **272**(5 Pt 1):C1482-91. doi:10.1152/ajpcell.1997.272.5.C1482

74. Lingueglia E, Renard S, Waldmann R, Voilley N, Champigny G, Plass H, et al. Different homologous subunits of the amiloride-sensitive Na+ channel are differently regulated by aldosterone. *J Biol Chem* (1994) **269**.

75. Hughey RP, Bruns JB, Kinlough CL, Harkleroad KL, Tong Q, Carattino MD, et al. Epithelial sodium channels are activated by furin-dependent proteolysis. *J. Biol. Chem.* (2004) **279**(18):18111–4. doi:10.1074/jbc.C400080200

76. Caldwell RA, Boucher RC, Stutts MJ. Serine protease activation of near-silent epithelial Na+ channels. *Am J Physiol Cell Physiol* (2004) **286**(1):C190-4. doi:10.1152/ajpcell.00342.2003

77. Shipway A, Danahay H, Williams JA, Tully DC, Backes BJ, Harris JL. Biochemical characterization of prostasin, a channel activating protease. *Biochem Biophys Res Commun* (2004) **324**(2):953–63. doi:10.1016/j.bbrc.2004.09.123

78. Passero CJ, Mueller GM, Rondon-Berrios H, Tofovic SP, Hughey RP, Kleyman TR. Plasmin activates epithelial Na+ channels by cleaving the gamma subunit. *J. Biol. Chem.* (2008) **283**(52):36586–91. doi:10.1074/jbc.M805676200

79. Kleyman TR, Carattino MD, Hughey RP. ENaC at the cutting edge: regulation of epithelial sodium channels by proteases. *J Biol Chem* (2009) **284**(31):20447–51. doi:10.1074/jbc.R800083200

80. Hughey RP, Bruns JB, Kinlough CL, Kleyman TR. Distinct pools of epithelial sodium channels are expressed at the plasma membrane. *J. Biol. Chem.* (2004) **279**(47):48491–4. doi:10.1074/jbc.C400460200

81. Vallet V, Chraibi A, Gaeggeler HP, Horisberger JD, Rossier BC. An epithelial serine protease activates the amiloride-sensitive sodium channel. *Nature* (1997) **389**(6651):607–10. doi:10.1038/39329

82. Snyder PM. Liddle's syndrome mutations disrupt cAMP-mediated translocation of the epithelial Na(+) channel to the cell surface. *J Clin Invest* (2000) **105**(1):45–53. doi:10.1172/JCI7869

83. Palmer LG, Frindt G. Gating of Na channels in the rat cortical collecting tubule: Effects of voltage and membrane stretch. *J Gen Physiol* (1996) **107**(1):35–45.

84. Palmer LG, Frindt G. Amiloride-sensitive Na channels from the apical membrane of the rat cortical collecting tubule. *Proc Natl Acad Sci U S A* (1986) **83**(8):2767–70. doi:10.1073/pnas.83.8.2767

85. Chraïbi A, Horisberger J-D. Na Self Inhibition of Human Epithelial Na Channel. *J Gen Physiol* (2002) **120**(2):133–45. doi:10.1085/jgp.20028612

86. Snyder PM. Minireview: Regulation of epithelial Na+ channel trafficking. *Endocrinology* (2005) **146**(12):5079–85. doi:10.1210/en.2005-0894

87. Collier DM, Snyder PM. Identification of epithelial Na+ channel (ENaC) intersubunit Cl- inhibitory residues suggests a trimeric alpha gamma beta channel architecture. *J Biol Chem* (2011) **286**(8):6027–32. doi:10.1074/jbc.M110.198127

88. Sheng S, Perry CJ, Kleyman TR. Extracellular Zn2+ activates epithelial Na+ channels by eliminating Na+ self-inhibition. *J. Biol. Chem.* (2004) **279**(30):31687–96. doi:10.1074/jbc.M405224200

89. Collier DM, Snyder PM. Extracellular protons regulate human ENaC by modulating Na+ self-inhibition. *J. Biol. Chem.* (2009) **284**(2):792–8. doi:10.1074/jbc.M806954200

90. Satlin LM, Sheng S, Woda CB, Kleyman TR. Epithelial Na(+) channels are regulated by flow. *Am J Physiol Renal Physiol* (2001) **280**(6):F1010-8. doi:10.1152/ajprenal.2001.280.6.F1010

91. Carattino MD, Sheng S, Kleyman TR. Epithelial Na+ channels are activated by laminar shear stress. *J. Biol. Chem.* (2004) **279**(6):4120–6. doi:10.1074/jbc.M311783200

92. Abi-Antoun T, Shi S, Tolino LA, Kleyman TR, Carattino MD. Second transmembrane domain modulates epithelial sodium channel gating in response to shear stress. *Am J Physiol Renal Physiol* (2011) **300**(5):F1089-95. doi:10.1152/ajprenal.00610.2010

93. Fronius M, Bogdan R, Althaus M, Morty RE, Clauss WG. Epithelial Na+ channels derived from human lung are activated by shear force. *Respir Physiol Neurobiol* (2010) **170**(1):113–9. doi:10.1016/j.resp.2009.11.004

94. Dagenais A, Fréchette R, Yamagata Y, Yamagata T, Carmel J-F, Clermont M-E, et al. Downregulation of ENaC activity and expression by TNF-alpha in alveolar epithelial cells. *Am J Physiol Lung Cell Mol Physiol* (2004) **286**(2):L301-11. doi:10.1152/ajplung.00326.2002

95. Czikora I, Alli A, Bao H-F, Kaftan D, Sridhar S, Apell H-J, et al. A novel tumor necrosis factor-mediated mechanism of direct epithelial sodium channel activation. *Am J Respir Crit Care Med* (2014) **190**(5):522–32. doi:10.1164/rccm.201405-0833OC

96. Shabbir W, Scherbaum-Hazemi P, Tzotzos S, Fischer B, Fischer H, Pietschmann H, et al. Mechanism of action of novel lung edema therapeutic AP301 by activation of the epithelial sodium channel. *Mol Pharmacol* (2013) **84**(6):899–910. doi:10.1124/mol.113.089409

97. Montesano R, Soulié P, Eble JA, Carrozzino F. Tumour necrosis factor alpha confers an invasive, transformed phenotype on mammary epithelial cells. *J Cell Sci* (2005) **118**(Pt 15):3487–500. doi:10.1242/jcs.02467

98. Lucas R, Magez S, Leys R de, Fransen L, Scheerlinck JP, Rampelberg M, et al. Mapping the lectin-like activity of tumor necrosis factor. *Science* (1994) **263**(5148):814–7.

99. Prof. Dr. Bernhard Fischer, CEO. *Apeptico and Mediolanum sign a Research & Development Cooperation and License Agreement for APEPTICO's therapeutic peptide Solnatide*. Vienna and Milano (2016).

100. Prof. Dr. Bernhard Fischer, CEO. *APEPTICO's development compounds Solnatide has been granted Orphan Drug Designation for "Treatment of Primary Graft Dysfunction following Lung Transplantation" and "Treatment of Pseudohypoaldosteronism Type 1B" by the Food and Drug Administration*. Vienna (2016).

101. Prof. Dr. Bernhard Fischer, CEO. *The Committee for Orphan Medicinal Products of the European Medicines Agency grants orphan drug designation to APEPTICO's development compounds AP301 and AP318 for treatment of for treatment of Pseudohypoaldosteronism Type 1B*. Vienna (2016).

102. Greig ER, Boot-Handford RP, Mani V, Sandle GI. Decreased expression of apical Na+ channels and basolateral Na+, K+-ATPase in ulcerative colitis. *J Pathol* (2004) **204**(1):84–92. doi:10.1002/path.1613

103. Nam HK, Nam MH, Kim HR, Rhie YJ, Yoo KH, Lee KH. Clinical Manifestation and Molecular Analysis of Three Korean Patients with the Renal Form of Pseudohypoaldosteronism Type 1. *Annals of Clinical and Laboratory Science* (2017) (47):83–7.

104. Gründer S, Rossier B. C. A reappraisal of aldosterone effects on the kidney: new insights provided by epithelial sodium channel cloning. *Curr Opin Nephrol Hypertens* (1997) **6**(1):35–9.

105. Kuhnle U. Pseudohypoaldosteronism: mutation found, problem solved? *Molecular and Cellular Endocrinology* (1997) (133):77–80.

106. Hanukoglu A, Bistritzer T, Rakover Y, Mandelberg A. Pseudohypoaldosteronism with increased sweat and saliva electrolyte values and frequent lower respiratory tract infections mimicking cystic fibrosis. *J Pediatr* (1994) **125**(5 Pt 1):752–5.

107. Saxena A, Hanukoglu I, Saxena D, Thompson RJ, Gardiner RM, Hanukoglu A. Novel mutations responsible for autosomal recessive multisystem pseudohypoaldosteronism and sequence variants in epithelial sodium channel alpha-, beta-, and gamma-subunit genes. *J Clin Endocrinol Metab* (2002) **87**(7):3344–50. doi:10.1210/jcem.87.7.8674

108. Strautnieks SS, Thompson RJ, Hanukoglu A, Dillon MJ, Hanukoglu I, Kuhnle U, Seckl J, Gardiner RM, Chung E. Localisation of pseudohypoaldosteronism genes to chromosome 16p12.2-13.11 and 12p13.1-pter by homozygosity mapping. *Hum Mol Genet* (1996) **5**(2):293–9.

109. Voilley N, Bassilana F, Mignon C, Merscher S, Mattéi MG, Carle GF, et al. Cloning, chromosomal localization, and physical linkage of the beta and gamma subunits (SCNN1B and SCNN1G) of the human epithelial amiloride-sensitive sodium channel. *Genomics* (1995) **28**(3):560–5. doi:10.1006/geno.1995.1188

110. Chang SS, Grunder S, Hanukoglu A, Rösler A, Mathew PM, Hanukoglu I, et al. Mutations in subunits of the epithelial sodium channel cause salt wasting with hyperkalaemic acidosis, pseudohypoaldosteronism type 1. *Nat Genet* (1996) **12**(3):248–53. doi:10.1038/ng0396-248

111. Gründer S, Firsov D, Chang SS, Jaeger NF, Gautschi I, Schild L, et al. A mutation causing pseudohypoaldosteronism type 1 identifies a conserved glycine that is involved in the gating of the epithelial sodium channel. *EMBO J* (1997) **16**(5):899–907. doi:10.1093/emboj/16.5.899

112. Botero-Velez M, Curtis JJ, Warnock DG. Brief report: Liddle's syndrome revisited--a disorder of sodium reabsorption in the distal tubule. *N Engl J Med* (1994) **330**(3):178–81. doi:10.1056/NEJM199401203300305

113. Shimkets RA, Warnock DG, Bositis CM, Nelson-Williams C, Hansson JH, Schambelan M, et al. Liddle's syndrome: Heritable human hypertension caused by mutations in the β subunit of the epithelial sodium channel. *Cell* (1994) **79**(3):407–14. doi:10.1016/0092-8674(94)90250-X

114. Rommens JM, Dho S, Bear CE, Kartner N, Kennedy D, Riordan JR, et al. cAMP-inducible chloride conductance in mouse fibroblast lines stably expressing the human cystic fibrosis transmembrane conductance regulator. *Proc Natl Acad Sci U S A* (1991) **88**(17):7500–4.

115. Boucher RC. New concepts of the pathogenesis of cystic fibrosis lung disease. *Eur Respir J* (2004) **23**(1):146–58.

116. Hummler E, Barker P, Gatzy J, Beermann F, Verdumo C, Schmidt A, et al. Early death due to defective neonatal lung liquid clearance in alpha-ENaC-deficient mice. *Nat Genet* (1996) **12**(3):325–8. doi:10.1038/ng0396-325

117. Kerem E, Bistritzer T, Hanukoglu A, Hofmann T, Zhou Z, Bennett W, et al. Pulmonary epithelial sodium-channel dysfunction and excess airway liquid in pseudohypoaldosteronism. *N Engl J Med* (1999) **341**(3):156–62. doi:10.1056/NEJM199907153410304

118. Chu S. *Sodium channel ENaC expression in lung epithelia* (2008). Available from: http://www.scitopics.com/Sodium_channel_ENaC_expression_in_lung_epithelia.html

119. Scherrer U, Sartori C, Lepori M, Allemann Y, Duplain H, Trueb L, et al. High-altitude pulmonary edema: From exaggerated pulmonary hypertension to a defect in transepithelial sodium transport. *Adv Exp Med Biol* (1999) **474**:93–107.

120. Knöpp Fenja. *Die Beteiligung der Extrazellulären Matrix an der Mechanosensitivität des humanen Epithelialen Na+ -Kanals (ENaC)*. Dissertation. Gießen (2014).

121. Schild L. The epithelial sodium channel and the control of sodium balance. *Biochim Biophys Acta* (2010) **1802**(12):1159–65. doi:10.1016/j.bbadis.2010.06.014

122. Lucas R, Yue Q, Alli A, Duke BJ, Al-Khalili O, Thai TL, et al. The Lectin-like Domain of TNF Increases ENaC Open Probability through a Novel Site at the Interface between the Second Transmembrane and C-terminal Domains of the α-Subunit. *J Biol Chem* (2016) **291**(45):23440–51. doi:10.1074/jbc.M116.718163

123. Kashlan OB, Adelman JL, Okumura S, Blobner BM, Zuzek Z, Hughey RP, et al. Constraint-based, homology model of the extracellular domain of the epithelial Na+ channel α subunit reveals a mechanism of channel activation by proteases. *J Biol Chem* (2011) **286**(1):649–60. doi:10.1074/jbc.M110.167098

124. Schaedel C, Marthinsen L, Kristoffersson A-C, Kornfält R, Nilsson KO, Orlenius B, et al. Lung symptoms in pseudohypoaldosteronism type 1 are associated with deficiency of the α-subunit of the epithelial sodium channel. *The Journal of Pediatrics* (1999) **135**(6):739–45. doi:10.1016/S0022-3476(99)70094-6

125. Welzel M, Akin L, Büscher A, Güran T, Hauffa BP, Högler W, et al. Five novel mutations in the SCNN1A gene causing autosomal recessive pseudohypoaldosteronism type 1. *Eur J Endocrinol* (2013) **168**(5):707–15. doi:10.1530/EJE-12-1000

126. Wang J, Yu T, Yin L, Li J, Yu L, Shen Y, et al. Novel mutations in the SCNN1A gene causing Pseudohypoaldosteronism type 1. *PLoS ONE* (2013) **8**(6):e65676. doi:10.1371/journal.pone.0065676

127. Stockand JD, Staruschenko A, Pochynyuk O, Booth RE, Silverthorn DU. Insight toward epithelial Na + channel mechanism revealed by the acid-sensing ion channel 1 structure. *IUBMB Life* (2008) **60**(9):620–8. doi:10.1002/iub.89

128. Adachi M, Tachibana K, Asakura Y, Abe S, Nakae J, Tajima T, et al. Compound heterozygous mutations in the gamma subunit gene of ENaC (1627delG and 1570-1G--A) in one sporadic Japanese patient with a systemic form of pseudohypoaldosteronism type 1. *J Clin Endocrinol Metab* (2001) **86**(1):9–12. doi:10.1210/jcem.86.1.7116

129. thermofisher.com. *Biotinylation*. Available from: https://www.thermofisher.com/at/en/home/life-science/protein-biology/protein-biology-learning-center/protein-biology-resource-library/pierce-protein-methods/biotinylation.html

130. thermofisher.com. *Avidin, NeutrAvidin and Streptavidin Conjugates—Section 7.6*. Available from: https://www.thermofisher.com/at/en/home/references/molecular-probes-the-handbook/antibodies-avidins-lectins-and-related-products/avidin-streptavidin-neutravidin-and-captavidin-biotin-binding-proteins-and-affinity-matrices.html

131. rockland-inc.com. *Biotin, Avidin, & Streptavidin: Technical Tips for Success*. Available from: https://rockland-inc.com/streptavidin-biotin-tips.aspx

132. Ruffieux-Daidié D, Poirot O, Boulkroun S, Verrey F, Kellenberger S, Staub O. Deubiquitylation regulates activation and proteolytic cleavage of ENaC. *J Am Soc Nephrol* (2008) **19**(11):2170–80. doi:10.1681/ASN.2007101130